

Annual Progress Report (APR)

Period of Report : 11.11.2020 till 31.07.2022

Annual Report (circle appropriate year): First Year / Second Year / Third Year

1. Title of Research Project: Investigation of the accretion flow properties of black hole binaries with AstroSat
- 2 (i) Name & Designation of the PI: Dr. Biplob Sarkar (Assistant Professor)
(ii) Phone/Fax/E-mail: 9101614336, biplobs@tezu.ernet.in, mails.biplob@gmail.com
(iii) Name & address of the Institution: Tezpur University, Napaam, Sonitpur,
Assam-784 028, INDIA
3. DOS Sanction Order No. and Date: No. DS_2B-13013(2)/2/2019-Sec.2
Dated April 23, 2019
4. Starting date of the project: April 23, 2019
5. Scientific Objectives:

Even though the proposal did target black hole binaries, during the course of the project work, the scientific objectives shifted to exploring neutron star (NS) X-ray binaries (XRBs). The Soft X-ray Telescope (SXT) instrument on-board AstroSat is sensitive to soft X-rays in the energy range of 0.3-8 keV. At the same time, the Large Area X-ray Proportional Counter (LAXPC) instrument observes astrophysical objects in the 3-80 keV X-ray band. LAXPC also has a fine time resolution of 10 microseconds, enabling it to monitor phenomena like rapid bursts. Taking these features of SXT and LAXPC instruments into consideration, the scientific objectives of the study of two different NS low mass X-ray binary (LMXB) sources carried out in the project are mentioned below:

WORK-I (Obs. ID: A04_122T01_9000002064)

- To report the detection of a Type-1 X-ray burst from the LMXB GX 3+1 with AstroSat, India's first multi-wavelength mission.
- To report the detection of the double-peak feature in the burst at higher energies.
- To present spectral analysis of the burst and report the physical parameters such as the blackbody temperature, the blackbody flux and the radius of the NS photosphere.

WORK-II (Obs. ID: G05_140T01_9000000628)

- To present the broadband X-ray data analysis using AstroSat of transient NS LMXB 4U 1608-52, which shows occasional outbursts.
- To perform a detailed timing and spectral study of the source using the observations made with AstroSat.
- To obtain physical insights into the evolution of accretion geometry in this system.

Biplob Sarkar
07/03/2024

6. Summary of the work carried out in the project during the current year

In the project during the current year, we have focussed on the accretion physics of NS XRBs and NS surface physics. In the first work, we investigated the AstroSat observation of GX 3+1 (Obs. ID: A04_122T01_9000002064), a NS XRB source detected with a bright burst from the stellar surface. We performed the modeling of the source spectra and calculated the source's physical parameters, such as the distance, luminosity, and radius of the NS. The burst from GX 3+1 is found to be a Type-1 thermonuclear burst, which is also a photospheric radius expansion burst. We have shown the evolution of the source radius with burst decay and estimated the NS's radius in the source, assuming the burst is isotropic. Utilising the burst parameters obtained, we provide a new estimation to the source distance, which is $\sim 9.3 \pm 0.4$ kpc, calculated for an isotropic burst emission.

In the second work, we present the broadband results from the study of a NS LMXB 4U 1608-52. The source was observed for an exposure time of around 40 ks with AstroSat (Obs. ID: G05_140T01_9000000628). The long-term Swift-BAT (15-50 keV) and MAXI (2-20 keV) light curves reveals that the position of AstroSat observation for the source is deviated from the peak in both cases. This gives us a preliminary hint that the source was in the hard-intermediate state during the AstroSat observation period. Analysis of the hardness intensity diagram shows that there is a strong positive correlation between source intensity and hardness. Therefore, we perform flux-resolved spectroscopy on the data extracted from SXT, LAXPC 10 and LAXPC 20 counters. The X-ray continuum can be satisfactorily explained using an absorbed thermal Comptonized model together with a blackbody component, but residuals are observed around 6.4 keV, which indicates the presence of Fe-line emission characteristics. Our timing analysis reveals a positive correlation of the fractional r.m.s power with energy bands of increasing energies. We find significant evolution in the photon index with the X-ray flux whereas the electron temperature is found to remain approximately constant. We discuss the implication of our findings on the changes in accretion geometry of the source with the X-ray flux.

7. Details of work done and results obtained during the period of the report

The details of work done and results obtained related to the two works during the period of the report are mentioned below:

WORK-I (Obs. ID: A04_122T01_9000002064)

- We have investigated the results of an observation of LMXB GX 3+1 with AstroSat's LAXPC and SXT instruments on-board for the first time.
- We have detected one Type-1 thermonuclear burst (~ 15 s) present in the LAXPC 20 light curve, with a double peak feature at higher energies.
- Our study of the hardness-intensity diagram reveals that the source was in a soft banana state.
- The pre-burst emission could be described well by a thermally Comptonised model component.

Biplob Sarkar
07/03/2024

- The burst spectra is modeled adopting a time-resolved spectroscopic method using a single color black-body model added to the pre-burst model, to monitor the parametric changes as the burst decays.
- On the basis of our time-resolved spectroscopy, we claim that the detected burst is a photospheric radius expansion burst.
- On the basis of literature surveys, we infer that AstroSat/LAXPC 20 has detected a burst from GX 3+1 after more than a decade, which is also a photospheric radius expansion one.
- Utilizing the burst parameters obtained, we provide a new estimation of the source distance, which is $\sim 9.3 \pm 0.4$ kpc, calculated for an isotropic burst emission.

WORK-II (Obs. ID: G05_140T01_9000000628)

- We have investigated the broadband results from the study of a NS LMXB 4U 1608-52, which was observed for an exposure time of around 40 ks with AstroSat.
- Based on our flux resolved spectroscopy, we could provide the evolution of physical parameters of the accretion disk.
- The electron temperature kT_e is found to remain constant ~ 2.9 keV with increase of photon flux intensity.
- The photon index is found to lower down with the photon flux intensity, from ~ 2.26 to ~ 1.85 .
- This shows the increase of hard photon flux in the spectra.
- The time lag is found to vary at different energies without any distinctive correlation.
- The fractional r.m.s shows a positive correlation with energy for frequency of 0.09 Hz where the power rises upto 3% beyond 20 keV.
- We estimate that the disk optical depth has shown a slight increment with the source count rate.

Conferences and webinars attended:

- (a) The Principal Investigator (PI) participated and presented an Oral Paper entitled "*AstroSat observation of rapid Type-I thermonuclear burst from the low mass X-ray binary GX 3+1*" in the *National Conference on Emerging Trends in Physics (NCETP 2021)* organized by Department of Physics, Tezpur University, Assam, India held on 16 June, 2021.
- (b) The PI presented a poster entitled "*AstroSat observations of the transient low-mass X-ray binary 4U 1608-52*" in *Two-days International Conference on Innovative Trends in Natural and Applied Sciences - 2021 (ICITNAS - 2021)* organized by Mahatma Gandhi College Of Science, Gadchandur, Tah. Korpana, Dist. Chandrapur- 442908 (M.S.), India on 17 -18 August, 2021.

Biplab Sarkar
07/03/2024

(c) The PI participated and presented an Oral Paper entitled "*Probing the accretion flow properties of NS LMXB 4U 1608-52 using AstroSat observations*", Biplob Sarkar, in *21st National Space Science Symposium*, January 31 - February 4, 2022, organized by IISER Kolkata, India.

(d) The PI presented a poster entitled "*Broad-band spectral and temporal characteristics of NS LMXB 4U1608-52 through AstroSat observations*" in the *40th Annual Meeting of the Astronomical Society of India (ASI)*, hosted jointly by IIT Roorkee and ARIES Nainital during 25-29 March 2022.

8. Work proposed to be done during the next year:

NONE (*Due to planned closure of the project since currently there is no research fellow engaged under the project after the resignation of the JRF, Mr. Ankur Nath*).

9. List of Publications during the period

Acceptance of manuscript in Journal of Astrophysics and Astronomy

Our paper entitled "*AstroSat observation of rapid Type-I thermonuclear burst from the low mass X-ray binary GX 3+1*" has been accepted for publication in the *Journal of Astrophysics and Astronomy* on *15 June 2022*.

Authors: Ankur Nath, Biplob Sarkar, Jayashree Roy, Ranjeev Misra

The PI of this project submitted the accepted paper on arXiv. The link to the paper is provided - <http://arxiv.org/abs/2206.07450>

10. Research/other staff appointed for the project

(Please provide name, designation, date of appointment etc.)

Name: Mr. Ankur Nath

Designation: Junior Research Fellow (JRF), Department of Applied Sciences, Tezpur University.

Date of appointment at Tezpur University: 11/02/2021

Date of resignation from Tezpur University: 31/12/2021

Mr. Ankur Nath worked at ICFAI University Tripura as "Junior Research Fellow" under Department of Physics from 03/06/2019 to 31/03/2020.

11 (a) Grants approved during the period (as per ISRO approval) :

- Rs. 5,21,848.00 (*As per sanction order dated November 11 ,2020 during second year of the project*)
- Rs. 1,30,462.00 (*First quarter grant for second year project received by Tezpur University on December 30, 2020*)
- Rs. 3,46,836.00 (*Balance grant of second year project received by Tezpur University on December 24, 2021*)

Biplob Sarkar
07/03/2024

(b) Expenditure incurred for the above period : Rs. 309001.00 (11-NOV-2020 TO 31-JUL-2022)

11.1	Budget Head	ISRO approved amount for current year	Amount utilized for current year	Amount requested for next year
11.1.	Research staff: JRF/SRF/RA etc.	Rs 377298.00	Rs 303449.00	NIL
11.2	Equipment (Name & cost of individual equipment purchased)	NIL	NIL	NIL
11.3	Consumable and Supplies	NIL	NIL	NIL
11.4	Travel	NIL	NIL	NIL
11.5	Contingency	Rs 100000.00	Rs 5552.00	NIL
11.6	Others	NIL	NIL	NIL
	Total	Rs 477298.00	Rs 309001.00	NIL

Biplob Sarkar
23/08/2022
Signature of the Principal Investigator

Date: 23.08.2022

NB: Kindly enclose the Annual Expenditure Statement and Fund Utilisation Certificate duly authenticated by the concerned Institution / University Officer

Biplob Sarkar
07/03/2024

Investigation of the accretion flow properties of black hole binaries with AstroSat

Report submitted to Dr. Biplob Sarkar (Principal Investigator)

Tezpur University, Napaam - 784 028, Tezpur.

by

Ankur Nath (Junior Research Fellow)

Tezpur University, Napaam - 784 028, Tezpur.

Project funded by Department of Space, Government of India

No.DS_2B-13013(2)/2/2019-Sec.2



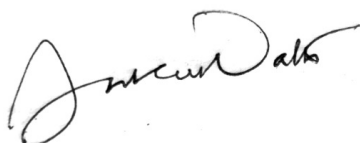
DEPARTMENT Of APPLIED SCIENCES

TEZPUR UNIVERSITY

Napaam, Sonitpur, Assam 784 028, India

Declaration

I declare that this written submission represents ideas in my own words, and wherever others' ideas and phrases have been included, I have adequately cited the sources down in the bibliography. I also declare that I have adhered to all academic honesty and integrity principles and have not misinterpreted, fabricated, or falsified any data/fact/source in my submission. I understand that any violation of the above will cause disciplinary actions by the Institute and can also evoke penal action from the sources I have thus not adequately cited or from whom proper permission has not been taken when needed.



Ankur Nath
Date. 18/07/2022

Certificate

This is to certify that the work contained in the written submission entitled “Investigation of the accretion flow properties of black hole binaries with AstroSat” submitted by Mr. Ankur Nath under the project No.DS_2B-13013(2)/2/2019-Sec.2, is a record of the candidate’s own work carried out by him under my supervision and guidance. The matter embodied in this report has not been submitted in part or full to any other university or institute for the award of any degree.

Biplob Sarkar
18/07/2022

Signature of Principal Investigator

Dr. Biplob Sarkar

Department of Applied Sciences,

Tezpur University,

Napaam, Sonitpur, Assam 784 028, India.

Abstract

This project aims to utilize the AstroSat data, an Indian spacecraft mission, and study the accretion disk physics of black hole binaries using the spacecraft's X-ray instrument data. However, during this work, my co-authors and I have found ourselves involved in neutron star data sets and the various phenomena happening in such sources. The prime reason for this track change is the non-availability of unique source data with features and clashes with parallel works on our targetted black hole data sets. As the research team got more involved in analyzing neutron stars, the main objective of this project got slightly modified. Thus, we have focussed on the accretion physics of neutron star X-ray binaries and neutron star surface physics and shifted ourselves off from black hole binaries. In the beginning, we discussed our proposed objectives to ISRO during the approval of the project and the achievements we could settle in after the project got accepted and funded duly by ISRO. After this short prelude, the main report begins. Our entire report consists of 4 chapters. In chapter 1, I talk about X-ray emission processes and their emergence in the field of astronomical research of X-ray binaries. I also discuss the Indian multiwavelength mission AstroSat and its payloads dedicated explicitly to X-ray astronomy. Chapter 2 consists of a report of AstroSat observation of GX 3+1, a neutron star X-binary source detected with a bright burst from the stellar surface. This report details the modeling of the source spectra and calculation of the source's physical parameters, such as the distance, luminosity, and radius of the neutron star. The final chapter 3 discusses another Astrosat observation of the X-ray binary 4U 1608-52. Data of the same source is analyzed, and detailed flux-resolved spectroscopy is carried out to investigate the change in the source's state detected during its temporal analysis. The respective chapters summarise the necessary discussions and physical interpretations of both works. The burst from GX 3+1 is found to be a Type 1 thermonuclear burst, which is also a photospheric expansion burst. We have shown the evolution of the source radius with burst decay and estimated the neutron star's radius in GX 3+1, assuming the burst is isotropic. Such bursts are considered bright enough to regard them as standard candles, and the luminosity of such radius expansion bursts could be used as a ruler to compute cosmic distances. We have noticed a change in optical depth of the accretion disk of the source 4U 1608-52, which is analyzed for a

parametric shift in corona temperature and the photon index of the disk during the evolution of the source's hardness with flux. The final chapter lists the conferences and webinars attended by the Principal Investigator (PI) and the Junior Research Fellow (JRF). During the COVID-19 pandemic, we attended online webinars and had our works noticed across various institutions in India.

Proposed vs. achieved objectives

The proposal

Recently, there has been a significant development in understanding the accretion process around a black hole. This has resulted from the significant developments in the theoretical front on the one hand and the improved observational capabilities on the other. The wide band coverage of the recent AstroSat mission has tremendously boosted the observational knowledge of black hole binaries. Again, the theoretical two-component accretion flow (TCAF) model has been found to explain many features of black hole candidates satisfactorily. Theoretical studies have also highlighted the importance of magnetic fields in the accretion process around a black hole. With such significant developments in both the theoretical and observational fronts, it is very pertinent to match the theoretical models with the observational findings of black hole sources. With this aim, the present proposal aims to utilize AstroSat archival data of black hole binaries, with a primary focus on the black hole sources H 1743-322, GRS 1716-249, XTE J1752-223, MAXI J1305-704, and GRS 1915+105. The archival data would be used to make a detailed study of these sources' spectral and temporal behavior, and the findings would be compared with the results from theoretical investigations. The uniqueness of the proposal lies in the fact that for the first time, we would perform phase-resolved spectroscopy with AstroSat, which has not been performed before. Also, we would attempt to generate the spectrum from the model based on magnetized accretion flow and fit it with the joint spectrum from SXT and LAXPC. We will be utilizing the excellent timing performance of LAXPC to study detailed timing properties of the source, including power density spectrum, quasi-periodic oscillation (QPO) features, and coherence between different energy bands. We will also be making use of the joint spectrum of SXT and LAXPC to understand the spectral characteristics of black hole binaries.

Proposed objectives

The objectives kept during the proposal of the project were

- Identification of various spectral components in the wide band X-ray spectra of the black

hole binaries using broad energy coverage in X-rays using joint spectrum from SXT and LAXPC.

- Phase-resolved spectroscopy for QPOs.
- A detailed study of the timing behavior of the sources using advanced timing techniques e.g., power spectral density, Fourier-frequency dependence of time lag, and coherence between different energy bands. The two software LAXPCSoft and GHATS will significantly help this task.
- Attempts will be made to interpret the spectral and timing characteristics from data with the models focusing on magnetized accretion flow. The observational results will also be interpreted with other models available in the literature for a comprehensive understanding of the source characteristics.
- Analysis of data for the proposed black hole binaries from other missions, e.g., Swift and NuSTAR, to complement the AstroSat data analysis, wherever required.

The expected results of the project were

- The wide coverage for X-ray spectroscopy will help investigate the continuum components present in the source. The two black hole binaries GRS 1716-249 and GRS 1915+105 have more than one observation from AstroSat. Attempts will be made to understand the relative variation of the spectral components (Keplerian or sub-Keplerian) from different observations in the AstroSat archive for the same source in terms of changing magnetic field strength in the accretion flow.
- New spectro-timing results are expected as an outcome of this work, considering the excellent timing resolution, larger collecting area of LAXPC, and broad coverage by SXT+LAXPC. We will be using advanced timing techniques on the energy-resolved time series to understand the detailed spectro-timing behavior of the sources.
- Since the background and calibration of LAXPC is not understood very well with 3% background uncertainty and 2% systematic uncertainty, we have chosen only brighter black hole binaries during outburst with MAXI counts > 0.1 counts s^{-1} in 2-20 keV band. The brightness of the sources is selected as one of the selection criteria while finalizing our sample of black hole binaries at this stage. This will help us get a better signal-to-noise ratio and allow the identification of spectral components and timing behavior in greater detail.
- Our attempts to understand the observed characteristics of the source in view of magnetized accretion flow models will help us developing a better understanding of accretion flow properties in black hole binaries.

- The results from the proposed study will be published in the journals of repute during the project duration.

Achievements

We want to highlight the fact that even though the proposal did target black hole binaries, during the course of the project work, we have come across the data of GX 3+1, which was detected with a prominent thermonuclear burst in it and was a neutron star (NS) X-ray binary. While studying its accretion properties, more focus was laid on investigating the burst from GX 3+1. We have checked on various black hole sources and collected their data, but we could discover the data had been already utilized along with their published reports. The practice session of the JRF involved timing analysis of QPOs from GX 1915+105, which has also aided in data analysis of GX 3+1 data. The Co-Investigator Dr. Anjali Rao had been the Observer of the GX 3+1 data for 9 LAXPC and SXT Orbits, and gradually our work shifted to exploring NS X-ray binaries. Our second work, which investigates the broadband analysis of the binary 4U 1608-52, is also an NS X-ray binary because the research competence developed by the JRF during the GX 3 + 1 investigation only focused on NS-specific investigations.

The achievements of our works are enlisted below

- We present the results of the AstroSat observation of the atoll type neutron star (NS) low-mass X-ray binary GX 3+1 performed on 2018 April 29-30. The source was observed with the LAXPC and SXT instruments onboard AstroSat and this observation was of total exposure of 100 ks ~ (ObsID: A04_122T01_9000002064)

- **AstroSat Observing Proposals Submitted:**

(i) **Proposal ID:** T03_121

Title: AstroSat ToO proposal for the X-ray transient MAXI J1348-630

PI: Biplob Sarkar

Co-Is: Anjali Rao & Jayashree Roy

Status: Rejected

(ii) **Proposal ID:** A09_032

Title: AstroSat AO proposal for Low Mass X-ray Binary GX 13+1

PI: Biplob Sarkar

Co-Is: Ankur Nath & Samuzal Barua

Status: Rejected

(iii) **Proposal ID:** A09_018

Title: AstroSat AO proposal for the X-ray transient GX 9+9

PI: Biplob Sarkar

Co-Is: Ankur Nath & Samuzal Barua

Status: *Accepted: full allocation*

- **Acceptance of manuscript in Journal of Astrophysics and Astronomy**

Our paper entitled “AstroSat observation of rapid Type-I thermonuclear burst from the low mass X-ray binary GX 3+1” has been accepted for publication in the Journal of Astrophysics and Astronomy on 15 June 2022. The PI of this project submitted the accepted paper on arXiv. The link to the paper is provided - <http://arxiv.org/abs/2206.07450>

List of Figures

2.1	The MAXI long time Light curve for GX 3+1 in the energy band 2-20 keV. The vertical line marks the <i>AstroSat</i> observation date.	27
2.2	<i>AstroSat</i> /LAXPC counter 20 light curve for ~ 100 ks data in the 3.0-80 keV energy band for a bin size of 1.0 seconds. A burst is observed at nearly 60 ks from the start of the observation with a sudden increment in the count rate by approximately 4 folds of the source's persistent count rate.	28
2.3	The upper and middle panels show source LAXPC 20 layer 1 light curves in the energy band 3-6 keV and 6-12 keV respectively. The bottom panel shows the hardness ratio $HR = \left(\frac{6-12 \text{ keV}}{3-6 \text{ keV}} \right)$. The binning size is 0.2 seconds. An increase in HR is seen during the burst, crossing 1.	29
2.4	The hardness-intensity diagram of GX 3+1. The hardness ratio (HR) is taken as the ratio of the count rates in energy bands 6-12 keV and 3-6 keV. The HR shows a positive correlation with the intensity. The plot is generated for a bin time of 60.0 s.	30
2.5	The plot shows the thermonuclear X-ray burst observed in different energy bands. The X-ray burst decays rapidly as energy approaches to 20 keV. The highest photon count is observed for the energy band 5-8 keV. All the light curves have a binning size of 0.2 s.	31
2.6	QDP modelling of the Type-1 burst. Fig.(a) shows modelling of the burst in 3-5 keV energy range, Fig.(b), in 5-8 keV energy range, Fig.(c) in 8-12 keV energy range and Fig.(d), models the burst light curve in 12-20 keV energy range. At higher energies, the double peaked feature is seen more distinctively.	32
2.7	The unfolded spectra from <i>AstroSat</i> for GX 3+1 (SXT spectrum in red and LAXPC 20 layer 1 spectrum in black). The top panel shows the spectra fitted with the model $\text{Constant} \times \text{TBABS} \times \text{NTHCOMP}$. The energy band used is 0.6 - 16.0 keV. The bottom panel shows the ratio of data and model.	33
2.8	The time bins selected for spectroscopy. The burst light curve shown here is in 8-12 keV energy band.	35

List of Figures

2.9 Time resolved spectroscopy of the burst using 5 time bins. We modelled the spectra during rise T1 shown by Fig.(a), Fig.(b), (c), (d) and (e) are the unfolded modelled spectra corresponding to the time bins T2, T3, T4, and T5. Each of the spectra is fitted following the conventional method on TBABS \times (NTHCOMP + BBODYRAD). NTHCOMP parameters are frozen at pre-burst values for all the spectra. 36

2.10 A combined plot of the evolution of unabsorbed flux, the normalisation constant of blackbody model, blackbody temperature kT_{bb} , the model error and the estimated photospheric radius in km for a source distance of 6.1 kpc. The x-axis counts the time from the rise of the burst. 37

3.1 The observation by *AstroSat* is marked with the black dotted line on MAXI (upper panel) and Swift/BAT (lower panel) daily light curves. *AstroSat* could capture it during its descent from an outburst 48

3.2 The light curve generated out of the total exposure data from laxpc 10 and 20 counters for a net energy range 3.0-80.0 keV (red), the background light curve of the same (green) and the final background subtracted light curve (blue). A binning time of 10 s is taken for all of the light curves. 49

3.3 The SXT light curve is shown here for an energy range 0.3-8.0 keV (red), A binning time of 2.3775 s is taken. 50

3.4 The Color Color Diagram of 4U 1608-52 with data from LAXPC 10 and 20 counters. 12.0 - 20.0 keV/6.0-12.0 is the Hard color ratio and 6.0-12.0/3.0-6.0 is the Soft color ratio. 51

3.5 The Hardness Intensity Diagram using data from the top layer of LAXPC 10 and 20. We observe a strong positive correlation of Hardness ratio (HR) with the intensity. The entire flux is sub-divided into four flux states- FS-1, FS-2, FS-3 and FS-4 based on increasing intensity. Each of these flux states are spectrally analysed ahead to study the spectral evolution of the source with increasing flux. 51

3.6 The evolution Hardness ratio of 4U 1608-52 with time. 52

3.7 Time lag of photons vs energy in 3-35 keV 53

3.8 Fractional rms vs energy in 3-35 keV 54

3.9 Flux resolved spectroscopy carried out using model combination Constant \times TBABS \times (GAUSS + THCOMP \times BLACKBODY). We have used LAXPC 10 (red), 20 (black) and SXT data (green). No redshift is considered. The THCOMP parameter photon convergence fraction is taken 100%. The spectral files are generated for the flux regions selected from the HID (see Fig. 3.5) 56

3.10 Evolution of spectral parameters with photon flux intensity in units of Counts/s selected from the Fig. 3.5. The photon index shows a decline whereas the electron temperature is fairly steady. The blackbody temperature shows a decline as well. No spectral correction factor is applied. 57

Contents

1 X-ray astronomy and AstroSat	17
1.1 Key investigations done with LMXB data	19
1.2 X-ray instruments in AstroSat	19
Bibliography	21
2 <i>AstroSat</i> observation of rapid Type-I thermonuclear burst from the low mass X-ray binary GX 3+1	23
2.1 Introduction	24
2.2 Observations and Data Reduction	26
2.2.1 <i>AstroSat</i> -SXT	27
2.2.2 <i>AstroSat</i> -LAXPC	27
2.3 Temporal Analysis	28
2.3.1 Search for Burst Oscillations	29
2.3.2 Energy-resolved burst profile	29
2.4 Spectral Analysis	31
2.4.1 Pre-burst Analysis	31
2.4.2 Burst Analysis	34
2.5 Discussions	35
Bibliography	41
3 Probing the accretion flow properties of NS LMXB 4U 1608-52 using <i>AstroSat</i> observations	45
3.1 Introduction	46
3.2 Data reduction and Temporal Analysis	48
3.2.1 Light curve	49
3.2.2 Color-Color and Hardness analysis	50

Contents

3.3	Timing analysis	52
3.4	Flux resolved spectroscopy	54
3.5	Discussions	56

Bibliography		59
---------------------	--	-----------

4	Conferences and webinars attended	61
----------	------------------------------------------	-----------

Chapter 1

X-ray astronomy and AstroSat

X-rays are a kind of electromagnetic radiation with frequencies substantially higher than visible light (3×10^{16} – 3×10^{19} Hz). In 1895, X-rays were detected for the first time, widely regarded as one of the most significant discoveries in history. While researching electric discharge events in gas, Wilhelm C. Roentgen covered the fluorescent screen with black cardboard and observed a faint glimmer. He dubbed these weird new photons X-rays, intending to give them a proper name later. X-rays are usually produced when electrons are accelerated at a high voltage.

X-rays from celestial sources were not discovered until after World War II, thanks to advances in rocket technology. Initially, it was assumed that objects in space could not produce X-rays stronger than those produced by the Sun. Even if they did, the Sun's X-ray radiation would obscure the X-rays. The first powerful cosmic source of X-rays was detected after a mission led by Riccardo Giacconi (Giacconi et al., 1962) was sent. This turning point drew the scientific community's attention to cosmic X-ray sources.

The four radiation mechanisms that produce astronomical X-rays are:

1. Thermal bremsstrahlung.
2. Synchrotron radiation.
3. Black body radiation.
4. Inverse Compton scattering.

Gases are ionized into electrons and positive ions at very high temperatures, generally around 10^5 K. When an electron collides with a positive ion in such an ionized medium, the two interact and cause the lighter electron to accelerate, causing it to change its direction. At temperatures above 10^6 K, electrons release energy during such accelerations, typically dominated by X-rays

1. X-ray astronomy and AstroSat

in astrophysical systems. The “bremsstrahlung” radiation is produced in this manner. The ionized medium usually reaches thermal equilibrium, and the emitted radiation is an energy continuum. However, the radiation sources in thermal gases may be a combination of bremsstrahlung and ‘line spectra.’ When rapid electrons collide with ions with bound electrons, energy is transferred, and a shift to higher energy states occurs. These excited ions decay swiftly to the ground state by shedding photons with energy equivalent to the energy level spacing through which the electrons stimulated them, resulting in line spectra.

A relativistic electron passing through a magnetic field is the second mechanism. The electromagnetic Lorentz force accelerates fast-moving electrons with a wide range of velocities, causing them to generate high-energy photons. Synchrotron radiation is the name given to this type of emission. The energy spectrum of the emission source, i.e., the electrons, has a power-law shape; hence the spectrum of synchrotron radiation usually has a power-law form as well. $I(E) = AE^\gamma$, where A is a constant and γ is the spectral index, yields the power law’s spectrum.

The blackbody emission is the third and dominant X-ray emission process. The frequency at which a blackbody emits is determined by its temperature. At temperatures over 10^6 K, X-rays dominate in the blackbody continuum spectra, and a common astrophysical example of such an emitting system is the surface of a star. Neutron stars release strong X-rays when accreting material touches the surface owing to blackbody radiation. (Seward & Charles, 1995). In astrophysics, inverse Compton scattering is an effective process for generating X-rays. The accretion disc surrounding a black hole or neutron star is thought to provide a thermal spectrum in X-ray astronomy. Relativistic electrons in the surrounding corona of the compact object scatter the lower energy photons produced by this spectrum to higher energies. The power law component in the X-ray spectra of accreting black holes is thought to be caused by this.

After this brief introduction of X-rays and their emission processes, we now draw attention to X-ray binaries. X-ray binaries are two-membered systems, with one member being a strong gravitational body (a black hole or neutron star) and the other orbiting it, usually a star known as the companion or donor star. These binaries are massive emitters of X-rays and the high luminosity results from energy loss from the stellar material spiraling onto the compact object from the companion star. Due to viscous processes, the accumulating material heats up. The details of these mechanisms are further highlighted in subsequent chapters. Astronomers have detected two types of X-ray binaries, i.e., High Mass X-ray Binary (HMXB) and Low Mass X-ray Binary (LMXB). The mechanisms through which these two kinds of sources emit X-rays are different and thus have an entire domain of research dedicated to these types individually. It is worth highlighting that the partner stars in HMXBs are big, and mass exchanges occur via stellar winds. The stars in LMXBs are not easily seen in the optical range due to their low mass, and the Roche-lobe mechanism determines the mass exchange. We would concentrate more on LMXBs from now onwards.

It has been discovered that LMXBs are the oldest members of binary stars at their final stage of stellar evolution. LMXBs are vital since we can well study physics near the neutron star or

the black hole from their accreting behavior. There are just a few hundred LMXBs detected, cataloged by Liu, van Paradijs, & van den Heuvel (2007)

1.1 Key investigations done with LMXB data

Below a list of features is provided which are an astronomer's first target to analyze an LMXB system:

1. Mass measurement: It is of enormous importance that the mass of the central body is measured because the critical argument in establishing the nature of the central body is whether the mass exceeds the upper limit ($\sim 3.0 M_{\odot}$) of the neutron star mass (Charles, 2011; Remillard et al., 2003).

2. We can analyze processes near neutron stars, e.g., X-ray bursts and kilohertz quasi-periodic oscillations kQPOs, burst oscillations to study the surface phenomena, the spin period, and the region near to coronal boundary. High-Frequency QPOs (HFQPOs) and Low-Frequency QPOs (LFQPOs) are detected from black hole binaries from regions near their event horizon. (Charles, 2011)

3. Most neutron star LMXBs are transient sources owing to the Roche-lobe filling mechanism of mass exchange. However, two distinct behaviors are detected from LMXBs based on which they are grouped into two categories, i.e., atoll and Z type. This is done when the patterns of the color-color diagrams are observed, which are closely connected to the source's spectral state.

4. X-ray bursts from atoll neutron star binaries can reach the Eddington limit, characterized by a neutron star's photospheric radius expansion (PRE). Their brightness could be used as standard candles for distance measurements, first proposed by van Paradijs (1978). Most short bursts are detected in a soft state of the sources.

5. The radius of the inner accretion disk could be estimated using a physical model, e.g., thermally Comptonised power-law models. The radii are calculated with the origin at the center of the compact object. The neutron star's radius is best calculated during the decay time of a PRE burst.

1.2 X-ray instruments in AstroSat

AstroSat is an Indian Astronomical mission launched in September 2015 with an initial operation plan of five years. Details of how data is reduced from *AstroSat* could be found in subsequent chapters but let us have a necessary introduction to the instruments of *AstroSat* dedicated to X-ray astronomy in particular.

- *AstroSat* can conduct surveys in different electromagnetic energy bands. The primary instruments for detecting X-rays in the ASTROSAT are the Soft X-ray Telescope (SXT) and the Large Area X-ray Proportional Counters (LAXPC) (Singh et al., 2014). SXT is

1. X-ray astronomy and AstroSat

for soft X-rays and has a detection range of 0.3-8 keV. LAXPC has three proportional counters with a detection range of 3-80 keV for hard X-ray observations.¹

- SXT performs spectroscopy of galactic plasma, supernovae remnants, clusters of galaxies, AGNs, accretion discs, and shocks, while the LAXPC studies the variability of X-ray sources. For hard X-ray imaging, another instrument is provided- the CZTI (Cadmium Zinc Telluride Imager) with energy sensitivity in the 10-250 keV region, and it is helpful in the spectroscopy of strong X-ray sources. The CZTI can also perform hard X-ray monitoring above 80 keV. Another instrument- Scanning Sky Monitor (SSM)- is present for detecting transient X-ray sources and is sensitive in the 2-10 keV energy band.²
- The LAXPC is made up of three large area proportional counters that are used to perform timing and broadband spectroscopy for variable astrophysical sources in the energy range of 3-80 keV X-rays. Large enclosures filled with gas and two electrodes kept at a potential differential make up proportional counters. The absorption of an X-ray photon in gas results in the generation of photoelectrons, which indicates that the X-ray photon has entered the gas. The potential difference causes additional multiplication by ionizing the gas atoms and creating more electrons. This causes a charge pulse to be detected, transformed to voltage, amplified, and measured between the electrodes.³
- The total effective area of the proportional counters of LAXPC is about 8000 cm² at the 5-30 keV energy band. The LAXPC equipment is unique because it can measure X-ray spectra over short time scales $\sim 10 \mu\text{s}$, so these counters are excellent instruments to capture fast astronomical events, e.g., abrupt outbursts from neutron star binaries which usually last for a few seconds.

As the picture is clear, mission *AstroSat* can simultaneously perform observations for wavelengths ranging from visible light to extremely hard X-rays. The satellite is thus an excellent telescope for observing the X-ray sky. It has a low inclination which leads to less contamination from background radiation. Unlike other X-ray satellites where detectors get saturated from bright X-ray sources, the SXT in *AstroSat* can detect bright sources reliably.

In the subsequent chapters, I intend to discuss reports of *AstroSat* observation of two atoll-type neutron star X-ray binaries. Chapter 2 analyzes a PRE burst detected from GX 3+1, a transient source with a compact neutron star. Chapter 3 consists of a report of *AstroSat* observation of 4U 1608-52, a neutron star binary detected with a variable hardness with source intensity.

¹ASTROSAT https://www.issdc.gov.in/docs/as1/AstroSat_Payloads.pdf

²https://www.tifr.res.in/~astrosat_sxt/index.html

³<https://www.isro.gov.in/astrosat/large-area-x-ray-proportional-counters-laxpc>

Bibliography

Charles P., 2011, ASPC, 447, 19

Liu Q. Z., van Paradijs J., van den Heuvel E. P. J., 2007, A&A, 469, 807

Remillard R., Munro M., McClintock J. E., Orosz J., 2003, nvm..conf, 57

Giacconi R., Gursky H., Paolini F. R., Rossi B. B., 1962, PhRvL, 9, 439

Seward F. D., Charles P. A., 1995, exru.book, 414

Singh K. P., Tandon S. N., Agrawal P. C., Antia H. M., Manchanda R. K., Yadav J. S., Seetha S.,
et al., 2014, SPIE, 9144, 91441S.

van Paradijs J., 1978, Natur, 274, 650.

Chapter 2

AstroSat observation of rapid Type-I thermonuclear burst from the low mass X-ray binary GX 3+1

Ankur Nath^{1,2}, Biplob Sarkar¹, Jayashree Roy³ and Ranjeev Misra³

¹Department of Applied Sciences, Tezpur University, Napaam-784028, Tezpur, Assam, India

²Faculty of Science & Technology, The ICFAI University Tripura, Agartala, 799210, India

³Inter-University Centre for Astronomy and Astrophysics (IUCAA), Post Bag 4, Ganeshkhind, Pune 411 007, India

Abstract

We report the results of an observation of low mass X-ray binary GX 3+1 with *AstroSat*'s Large Area X-ray Proportional Counter (LAXPC) and Soft X-ray Telescope (SXT) instruments on-board for the first time.¹ We have detected one Type-I thermonuclear burst (~ 15 s) present in the LAXPC 20 light curve, with a double peak feature at higher energies and our study of the hardness-intensity diagram reveals that the source was in a soft banana state. The pre-burst emission could be described well by a thermally Comptonised model component. The burst spectra is modelled adopting a time-resolved spectroscopic method using a single color blackbody model added to the pre-burst model, to monitor the parametric

¹The contents of this chapter are accepted for publication in Nath A., Sarkar B., Roy J., Misra R., 2022, Journal of Astrophysics and Astronomy.

2. *AstroSat* observation of rapid Type-I thermonuclear burst from the low mass X-ray binary GX 3+1

changes as the burst decays. Based on our time-resolved spectroscopy, we claim that the detected burst is a photospheric radius expansion (PRE) burst. During the PRE phase, the blackbody flux is found to be approximately constant at an averaged value ~ 2.56 in 10^{-8} ergs s^{-1} cm^{-2} units. On the basis of literature survey, we infer that *AstroSat*/LAXPC 20 has detected a burst from GX 3+1 after more than a decade which is also a PRE one. Utilising the burst parameters obtained, we provide a new estimation to the source distance, which is $\sim 9.3 \pm 0.4$ kpc, calculated for an isotropic burst emission. Finally, we discuss and compare our findings with the published literature reports.

Keywords— X-rays: binaries—stars: neutron—pulsars: individual: GX 3+1—X-rays: stars—methods: data analysis—*AstroSat*: LAXPC/SXT.

2.1 Introduction

The low mass X-ray binary (LMXB) GX 3+1 was first detected during an *Aerobee*-rocket flight on June 16, 1964 (Bowyer et al., 1965). LMXBs are binary systems which are older than $\sim 10^9$ years with their companion stars having mass $\leq 1 M_{\odot}$ (Bhattacharya & van den Heuvel, 1991; Verbunt, 1993). Ever since the discovery of LMXBs, which have neutron stars as compact objects, short thermonuclear bursts have been reported (Grindlay et al., 1976; Belian et al., 1976; Strohmayer & Bildsten, 2006; Galloway et al., 2020). X-ray bursts in LMXBs are marked as rapid rise in the photon count in the time scale of seconds followed by an exponential decay (Galloway et al., 2008). These are the nuclear runaway phenomena, which are caused by the accreted material from the companion falling onto the NS surface via Roche-lobe overflow mechanism. Pure or mixed hydrogen burns upto a critical density, beyond which bursts bright in X-rays occur locally - see reviews by Lewin et al. (1993), Strohmayer & Bildsten, (2006) and Bhattacharyya, (2010). Usually the decay times vary between ~ 10 -100 s as reported by Lewin, (1977); Hoffman et al., (1978); Lewin et al., (1993); Galloway et al. (2008). During spectral modelling, Type-1 bursts are normally described with blackbody models.

GX 3+1 is a persistently bright X-ray binary source. After eight years of its discovery, it was first detected with Type-1 short bursts, which indicated that the compact object at the center certainly has to be an NS (Makishima et al., 1983). As reported from the All Sky Monitor (ASM) observation (Levine et al., 1996), the average X-ray intensity of GX 3+1 is slowly varying over a time scale of months to years by a factor of ~ 2 with high X-ray luminosity (10^{37} - 10^{38} ergs s^{-1}) and non-periodic behaviour (Mondal et al., 2019).

Being a luminous, persistent source GX 3+1 has been observed by many major X-ray missions such as *Ginga* (Asai et al., 1993), *EXOSAT* (Schulz et al., 1989), *RXTE* (Bradt et al., 1993; Kuulkers & van der Klis, 2000), *BeppoSAX* (den Hartog et al., 2003), *INTEGRAL* (Chenevez et al., 2006; Paizis et al., 2006), *Chandra* (van den Berg et al., 2014), *XMM-Newton* (Pintore et al., 2015), *NuSTAR* (Mondal et al., 2019). This present work is based on the observation of GX 3+1 by mission *AstroSat*.

LMXBs are mainly grouped as Z or Atoll sources, based on the characteristic shapes they trace on their color-color diagrams (CCD). Atoll sources display mainly two tracks in hardness-intensity diagrams: the banana and island states. GX 3+1 has been reported to be a bright atoll source having a soft spectrum typically $\sim 2\text{-}10$ keV (Mondal et al., 2019). Ever since its discovery this source has been always found in banana state. Two branch structures were detected in its hardness intensity diagram (HID) which were identified as lower and upper banana states in the report by Asai et al. (1993). No island state has been observed so far from GX 3+1 and no kHz Quasi-periodic oscillations (QPOs) are detected. (Homan et al., 1998; Oosterbroek et al., 2001; Chenevez et al., 2006, Mondal et al., 2019).

Historically, GX 3+1 has shown doubly peaked bursts in 9-22 keV energy band reported by Makishima et al. (1983) which was the first report of Type-1 bursts from GX 3+1. Following this, GX 3+1 was found to be a very active X-ray burster and bursts were studied by Asai et al. (1993); Pavlinsky et al. (1994); Molkov et al. (1999). However, the first investigation of a double peak photospheric radius expansion burst (PRE) was carried out by Kuulkers & van der Klis (2000) using *RXTE* data. They had estimated the source distance to be between 4.2 - 6.4 kpc for an uncertainty of 30 %. A total of 61 bursts from GX 3+1 was reported by den Hartog et al. (2003) which were observed in a high state of the source. However, an exceptional superburst was reported by Kuulkers (2002) with *RXTE/ASM* data, which had a decay time of ~ 1.6 hours. An unusual intermediate burst with a duration of ~ 30 min was detected on 2004 by *INTEGRAL/JEM-X*, which was analysed by Chenevez et al. (2006). The same data set was re-evaluated by Alizai et al. (2020) using different spectral models. Thus, we find that no burst phenomenon has been reported for this source since 2004.

Thermonuclear X-ray bursts from GX 3+1 have never been reported earlier using AstroSat data. However, type-1 thermonuclear bursts has been detected by AstroSat previously from various LMXBs (Bhattacharyya et al., 2018; Beri et al., 2019; Devasia et al., 2021; Bhulla et al., 2020; Roy et al., 2021, Kashyap et al., 2022). PRE burst events for the LMXB 4U 1636-536 have been reported earlier using AstroSat data by Beri et al. (2019) and Roy et al. (2021).

The spectral fitting of NS bursts involve modelling with a single color blackbody component (Hoffman et al., 1977; Beri et al., 2019; Bhulla et al., 2020). The pre-burst spectrum of several LMXBs are found to be well fitted with a thermally Comptonized model, which describes the powerlaw behaviour of the energy (Pintore et al., 2015; Verdhan Chauhan et al., 2017; Bhattacharyya et al., 2018; Chen et al., 2019). The parameter values of the black-body model could be used to estimate the temperature near the NS surface $kT_{\text{bb}} > 1$ keV (Seifina & Titarchuk, 2012) and the physical radius of the NS. The model parameters evolve with time in rapid events like bursts, so it is needful to divide bursts into short time intervals and fit the spectra of each interval, from the rise to the decay of the burst, which is the conventional method of time-resolved spectroscopy (Lewin et al., 1993; Swank et al., 1977). The source's persistent pre-burst spectra is assumed to be unevolved during the burst and used to serve as the background spectrum for the burst spectra. This is the conventional method of burst spectral analysis. Since type-1

2. *AstroSat* observation of rapid Type-I thermonuclear burst from the low mass X-ray binary GX 3+1

bursts are highly luminous than the source's average photon count rate, so it is acceptable to consider modelling of the burst spectra distinguishably assuming the burst doesn't influence the background persistent emission. But reports have showed that bursts can modify the persistent spectra (Chen et al., 2012; in't Zand et al., 2013; Degenaar et al., 2018; Keek et al., 2018). Worpel et al. (2013, 2015) introduced the " f_a " (which is a scaling factor supplied to the persistent spectrum) method and reported the change in persistent flux due to the burst. When the " f_a " is fixed at unity, the model follows the conventional method.

The objectives of this chapter are summarised in the following: (i) reporting the detection of a type I X-ray burst from GX 3+1 with *AstroSat*, (ii) reporting the detection of the double-peak feature in the burst at higher energies, and, (iii) presenting spectral analysis of the burst and reporting the physical parameters such as the blackbody temperature, the blackbody flux and the radius of the NS photosphere.

The organization of this chapter is as follows- Section 2 discusses the observational details and mentions all the data reduction techniques briefly. Section 3 presents the light curve, the hardness ratio of the photon count rate, the hardness-intensity diagram (HID), an energy resolved burst light curve and QDP modelling of the burst at each energy band. We have performed a joint fitting of the persistent pre-burst spectrum, using SXT and LAXPC 20 data and obtained the parameter values for a thermally Comptonized component, elaborated in Section 4.1. We have adopted the conventional approach to fit model the burst, elaborated in Section 4.2. All the results are discussed and compared to highlight the consistencies with earlier published reports in Section 5.

2.2 Observations and Data Reduction

AstroSat is India's first multi-wavelength astronomy mission satellite launched on September 28, 2015. For dedicated studies on X-ray astronomy, *AstroSat* has been provided with payloads Soft X-ray focusing Telescope (SXT) and three Large Area X-Ray Proportional Counters (LAXPC) named as LAXPC 10, LAXPC 20 & LAXPC 30. *AstroSat* observed GX 3+1 in an Announcement of Opportunity (AO) observation conducted in April 29-30, 2018 (Obs ID:A04_122T01_9000002064). The observation was done for the Right Ascension (RA) $\alpha = 266.983329$ and Declination point (DEC) $\delta = -26.56361$ in International Celestial Reference System (ICRS), for the celestial co-ordinates of GX 3+1. The Observation by *AstroSat* is marked on the MAXI long time light curve in 2-20 keV shown in Fig. 1. The source was showing a persistent behaviour during the *AstroSat* observation, as it is evident from the MAXI light curve.

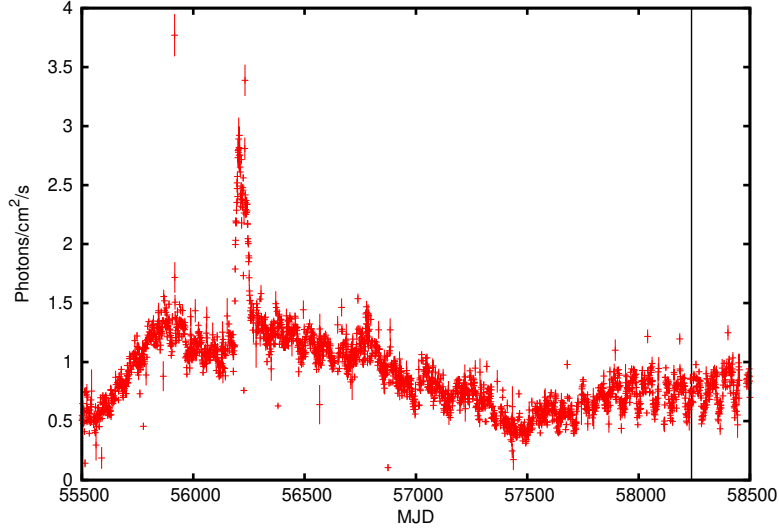


Figure 2.1: The MAXI long time Light curve for GX 3+1 in the energy band 2-20 keV. The vertical line marks the *AstroSat* observation date.

2.2.1 *AstroSat*-SXT

The SXT (Singh et al., 2016, 2017) has an operational energy band of 0.3-8.0 keV (Singh et al., 2017; Bhattacharyya et al., 2021). The SXT pipeline software² (version: AS1SXTLevel2-1.4b) is used to generate the Level 2 data of 9 orbits using the Photon Counting (PC) mode for Level 1 data. The SXT event merger script is used to merge the data for different orbits to produce the clean event file. An encircled region of radius 13.5 arcmin in physical coordinates is extracted which comprises $\sim 96\%$ of the source photons, for the generation of source spectrum. This extraction is done using the standard tools of XSELECT V2.4g. The light curve of minimum allowed time bin for SXT instrument i.e 2.3775 s, is thus obtained from this region file. The Auxillary Response File (ARF) is generated by using sxtARFModule³ tool of the ARF on-axis (version 20190608) provided by the SXT instrument team. The SXT spectrum file is used with a blank sky background spectrum provided by the SXT instrument team during our model fitting. No pile up is observed for the source. The energy band during the generation of the SXT spectrum file is kept the default 0.3-8.0 keV (Singh et al., 2017; Bhattacharyya et al., 2021).

2.2.2 *AstroSat*-LAXPC

LAXPC counters have been designed to detect X-ray photons of energies 3.0-80 keV (Yadav et al., 2016; Antia et al., 2021). With a total of three proportional counters as mentioned before, LAXPC has a total effective area of $\sim 8000 \text{ cm}^2$. Each of the three counters work independently to record photons with a time resolution of roughly $10 \mu\text{s}$. This makes LAXPC able to observe fast variability like thermonuclear bursts. We use the data only from LAXPC 20 because LAXPC

²<http://astrosat-ssc.iucaa.in/?q=sxtData>

³www.tifr.res.in/~astrosat_sxt

2. *AstroSat* observation of rapid Type-I thermonuclear burst from the low mass X-ray binary GX 3+1

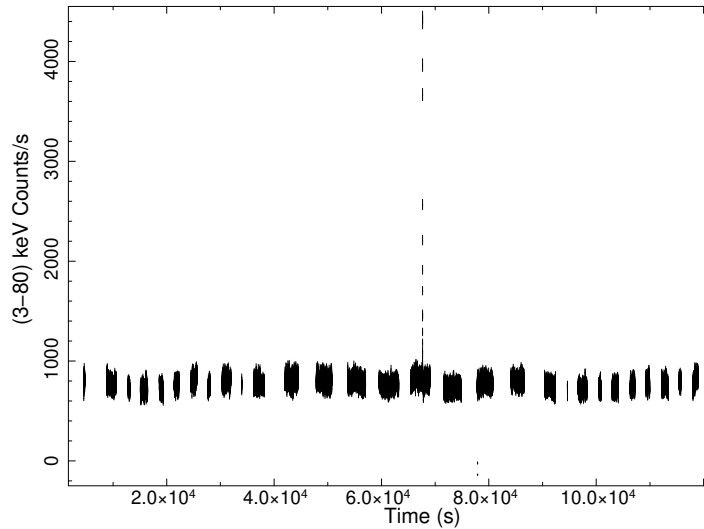


Figure 2.2: *AstroSat*/LAXPC counter 20 light curve for ~ 100 ks data in the 3.0-80 keV energy band for a bin size of 1.0 seconds. A burst is observed at nearly 60 ks from the start of the observation with a sudden increment in the count rate by approximately 4 folds of the source's persistent count rate.

10 has been found displaying instability in its response and LAXPC 30 is excluded as it has been officially shut down, at the time of observation of GX 3+1.

We have generated the Level 2 data of 9 orbits from LAXPC 20 using the Event Analysis (EA) mode. EA mode data contains the information about the time, anodeID and Pulse Height Amplitude (PHA) for each event. The processing of the LAXPC data is done using individual routine software *LaxpcSoft*⁴ version: May 19, 2018. We have only used the layer 1 (top layer) of the LAXPC 20 counter for the temporal and spectral analysis except for the full time light curve, which is generated using all the layers of the same counter.

2.3 Temporal Analysis

The LAXPC 20 light curve is generated for the good time intervals only. The background is subtracted for a default 2% systematic error. A nearly persistent photon count rate of ~ 1000 counts/s is observed from the light curve. As we cross about 60 ks from the observational start time, the burst feature is prominent (Fig. 2) with its photon count rate (~ 4000 counts/s) almost four times the non-burst rate.

The Fig. 3 shows the detected photons in LAXPC 20 layer 1 in energy bands 3-6 keV and 6-12 keV, with their respective light curves plotted simultaneously and the hardness ratio (HR) (6-12 keV/3-6 keV) of the two light curves in the bottom panel, with their corresponding hardness ratio shown at the bottom panel. The bin size is selected as 0.2 s. We have used *xronos* v5.22 is used to generate this multiplot. We can thus infer that during the entire observation period, the source is detected in a soft state since the average hardness ratio was $\sim 0.6-0.7$ during

⁴<http://astrosat-ssc.iucaa.in/?q=laxpcData>

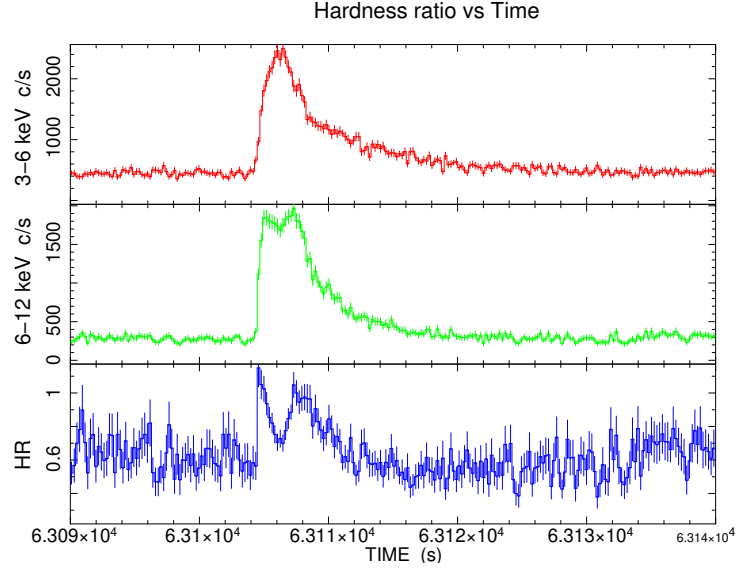


Figure 2.3: The upper and middle panels show source LAXPC 20 layer 1 light curves in the energy band 3-6 keV and 6-12 keV respectively. The bottom panel shows the hardness ratio $HR = \left(\frac{6-12 \text{ keV}}{3-6 \text{ keV}} \right)$. The binning size is 0.2 seconds. An increase in HR is seen during the burst, crossing 1.

the entire observation. But during the occurrence of the burst, we notice the ratio increases, crossing 1.0, followed a sharp drop in the hardness and a subsequent rise. As the burst decays, the ratio drops to the persistent level.

The HID is plotted as a function of source’s intensity (Fig. 4). For an HR (6-12 keV)/(3-6 keV) with a binning size of 60 seconds, we observe a positive correlation of the HR with source intensity in the energy band 3-12 keV. A positive correlation between hardness and intensity is also reported by Mondal et al. (2019) which indicates the characteristic soft banana state.

2.3.1 Search for Burst Oscillations

We have investigated the power density spectrum (PDS) to detect burst oscillations using data from LAXPC 20 all layers. To generate the PDS, we have used the Laxpcsoftware task “*laxpc_fnd_freqflag*” which outputs the power spectra as a function of frequency. These PDS are generated using a burst GTI file of 16 s exposure. We have also used the GTI file for the entire orbit data from LAXPC 20 all layers in which the burst has been detected and plotted the respective PDS upto 1000 Hz. We have also parallely used the ftool *powspec* 1.0 (XRONOS v 6.0) to generate PDS with binning of 0.005 s, 0.004 s, 0.003 s and 0.002 s. However, we could not detect any signal of oscillations.

2.3.2 Energy-resolved burst profile

To resolve the entire burst into separate energy bands, we generate four burst light curves in narrow energy bands: 3-5 keV, 5-8 keV, 8-12 keV and 12-20 keV. All of these light curves have

2. *AstroSat* observation of rapid Type-I thermonuclear burst from the low mass X-ray binary GX 3+1

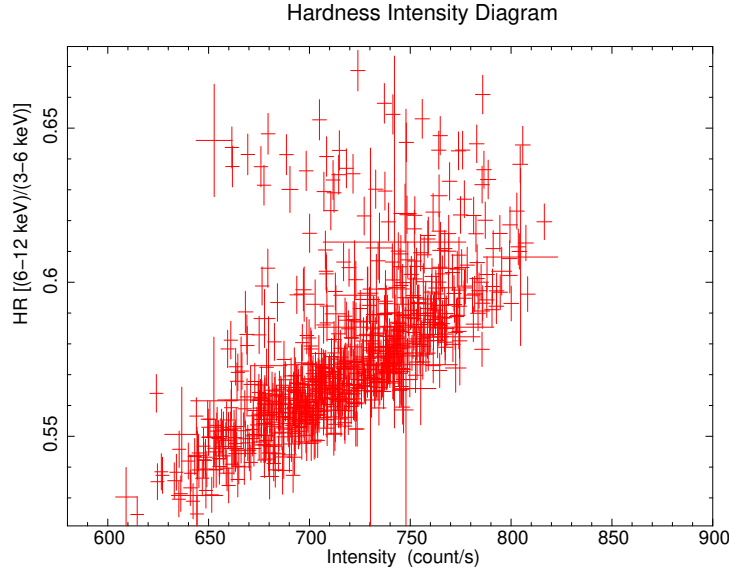


Figure 2.4: The hardness-intensity diagram of GX 3+1. The hardness ratio (HR) is taken as the ratio of the count rates in energy bands 6-12 keV and 3-6 keV. The HR shows a positive correlation with the intensity. The plot is generated for a bin time of 60.0 s.

Table 2.1: The duration of rise, peak to persistent count ratio, decay duration and flux at the burst peak estimated for four narrow energy bands of the burst. The count ratio is the approximate ratio of peak count rate and the persistent count rate, obtained for each *Burs* model

Energy band (keV)	Duration of rise(s)	Count ratio	Decay duration(s)	Peak Flux
3 - 5	0.845, 1.05	~ 3.18, 5.12	1.7, 6.81	9.763
5 - 8	0.72, 3.15	~ 6.96, 4.24	5.98, 1.56	11.471
8 - 12	0.52, 1.616	~ 8.03, 7.58	2.87, 1.89	8.430
12 - 20	0.4, 1.97	~ 10.43, 8.69	1.22, 1.59	5.270

The peak flux is in units of 10^{-9} ergs s^{-1} cm^{-2}

a binning size of 0.16 seconds. From Fig. 5, we observe the burst has the highest photon count rate in 5-8 keV band, crossing 2000 counts/s. This is followed by the light curves in 3-5 keV, 8-12 keV and 12-20 keV band in a descending order of photon count rate. The double peak feature is observed in the 8-12 keV and 12-20 keV bands. These burst light curves are generated after subtracting the background light curves, using a default systematic error of 2% for the LAXPC instrument and no scaling factors are multiplied. We have performed a measurement of the exponential decay times of the burst in four energy bands by fitting the corresponding light curves with a model combination of a constant added to QDP *Burs* model⁵ (Devasia et al., 2021). To achieve a better fitting, we include two *Burs* models. We show the model fits for four burst profiles in their respective energy bands in Fig. 6 and report the obtained rise time, the approximate ratio of the burst peak count rate and the persistent count rate and the decay time, in Table. 2.1. We find that the peak to persistent count rate ratio is higher for higher energy bands, as evident from Fig. 6(a-d). QDP *Burs* modelling of burst profile has been done previously by

⁵<https://heasarc.gsfc.nasa.gov/ftools/others/qdp/qdp.html>

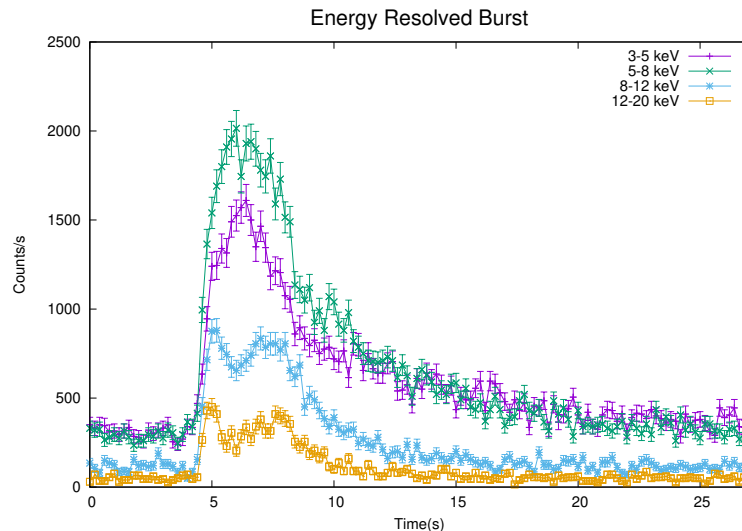


Figure 2.5: The plot shows the thermonuclear X-ray burst observed in different energy bands. The X-ray burst decays rapidly as energy approaches to 20 keV. The highest photon count is observed for the energy band 5-8 keV. All the light curves have a binning size of 0.2 s.

Marino et al. (2019), Beri et al. (2019) and Hu et al. (2020) to obtain their timing properties. The peak flux values listed in Table. 2.1 have been obtained by using the XSPEC command *flux* on the spectral files of exposure ~ 3 s near the peak of each of the energy resolved burst light curve.

2.4 Spectral Analysis

To perform the spectral fitting, we have used the SXT spectrum file, mentioned in Section 2.1. We have considered only layer 1 data from LAXPC 20 unit to obtain non-burst or pre-burst spectrum and the burst spectrum. We consider two broad regions of data - the pre-burst region and the burst region.

2.4.1 Pre-burst Analysis

The pre-burst energy spectrum of the source is obtained from the combined analysis of the SXT and LAXPC 20 layer 1 spectral data of ~ 841 s, which is modelled by a thermally Comptonized component NTHCOMP (Zdziarski et al., 1996; Życki et al., 1999) in XSPEC v12.10.1f (Arnaud, 1996). We choose an energy range with a lower limit at 0.6 keV because of the uncertainties in the response at lower energies and higher limit at 16 keV, since the spectra is found to be background dominated at higher energies. The XSPEC routine TBABS (Wilms et al., 2000) is used for taking the interstellar medium (ISM) absorption into account. We freeze the neutral hydrogen column density (N_{H}) at $1.4 \times 10^{22} \text{ cm}^{-2}$ (Fig. 7) which is close to the value $\sim 1.5 \times 10^{22} \text{ cm}^{-2}$ reported by Morrison & McCammon (1983). We select the input type 1 which considers that the seed photons are supplied to the corona by the accretion disk.

2. *AstroSat* observation of rapid Type-I thermonuclear burst from the low mass X-ray binary GX 3+1

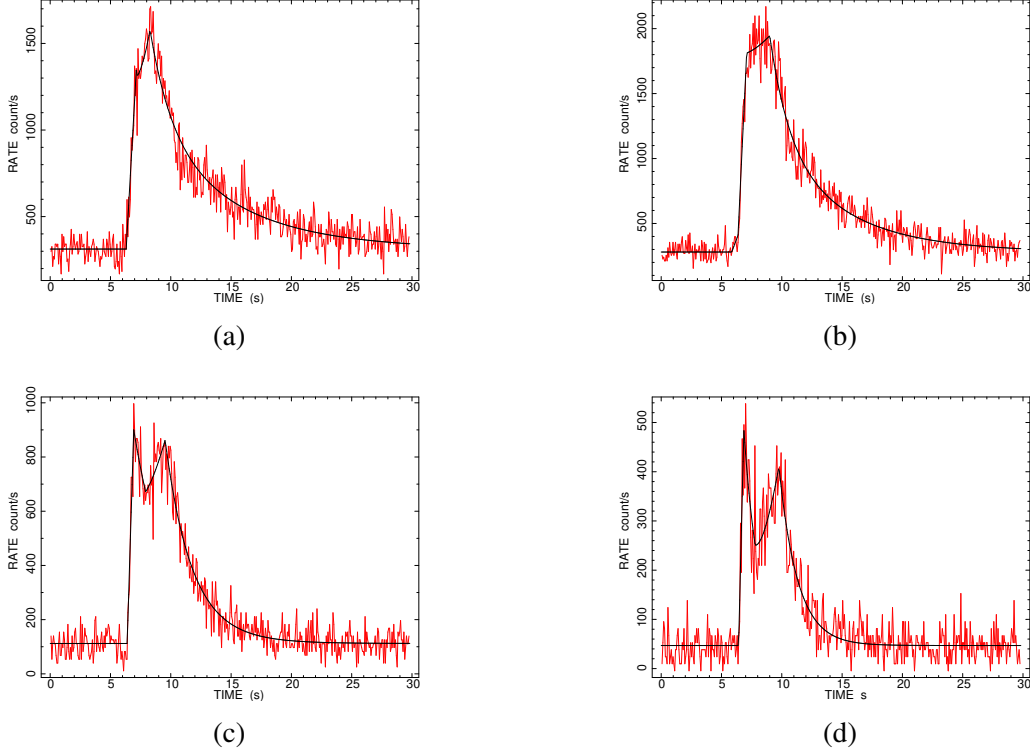


Figure 2.6: QDP modelling of the Type-1 burst. Fig.(a) shows modelling of the burst in 3-5 keV energy range, Fig.(b), in 5-8 keV energy range, Fig.(c) in 8-12 keV energy range and Fig.(d), models the burst light curve in 12-20 keV energy range. At higher energies, the double peaked feature is seen more distinctively.

Table. 2.2 shows all the parameter values achieved for the best fit. The LAXPC 20 layer 1 spectrum and the SXT spectrum are obtained for energy bands 4.0 - 16.0 keV and 0.6 - 7.0 keV respectively. The SXT spectrum's response file is provided a gain correction, with its slope frozen to 1.0 and its best fit offset obtained $\sim 0.047^{+0.008}_{-0.012}$. A systematic error of 3% is considered to account for the uncertainties in the response calibration⁶ (Maqbool et al., 2019; Mudambi et al., 2020).

While fitting, the photon index Γ is found to settle at $\sim 3.5 \pm 0.35$, which is in agreement with the reported values from Chenevez et al. (2006); Pintore et al. (2015); Ludlam et al. (2019). The electron temperature kT_e is obtained $\sim 4.46^{+2.55}_{-0.88}$ keV and the seed photon temperature kT_{nth} is achieved $\sim 1.82^{+0.07}_{-0.07}$ keV. The low value of the electron temperature indicates to the soft state of the source, which is in agreement with our obtained HID shown in Fig. 4. The fit attains a chi-squared value of 471.76 for 437 degrees of freedom, which is a good fitting. The SXT spectrum is rescaled by a constant factor $\sim 1.18^{+0.04}_{-0.04}$, while keeping the same constant fixed to 1.0 for LAXPC 20 layer 1 spectrum.

The unabsorbed flux is found to be slightly more for the SXT spectra in comparison to the LAXPC 20 layer 1 spectra (4.46 and 6.41 in units of 10^{-9} ergs s^{-1} cm^{-2} , for LAXPC and SXT

⁶https://www.tifr.res.in/~astrosat_sxt/dataana_up/readme_sxt_arf_data_analysis.txt

Table 2.2: The best-fit parameter values for the joint pre-burst spectral modelling of SXT and LAXPC 20 layer 1 data with a thermally Comptonized multicolour black-body Constant×TBABS×NTHCOMP. Errors are at 90% confidence range for each parameter

Component	Parameter(Unit)	LAXPC 20	SXT
TBABS	$N_{\text{H}}(10^{22} \text{ cm}^{-2})$	1.4 (frozen)	1.4 (frozen)
Constant		1.0 (frozen)	$1.18^{+0.04}_{-0.04}$
NTHCOMP	Γ^{α}	$3.5^{+0.4}_{-0.3}$	$3.5^{+0.4}_{-0.3}$
	$kT_e^{\beta}(\text{keV})$	$4.46^{+2.55}_{-0.88}$	$4.46^{+2.55}_{-0.88}$
	$kT_{\text{nth}}^{\gamma}(\text{keV})$	$1.82^{+0.07}_{-0.07}$	$1.81^{+0.07}_{-0.07}$
	N_{nth}^{δ}	$0.73^{+0.04}_{-0.04}$	$0.73^{+0.04}_{-0.04}$
Gain	Slope	-	(1.0)
	Offset (E-02)	-	$5.73^{+0.006}_{-0.007}$
	$\chi^2/\text{d.o.f}$	1.08	1.08
	$f^{\eta}(10^{-9} \text{ ergs s}^{-1} \text{ cm}^{-2})$	$4.46^{+0.1}_{-0.1}$	$6.41^{+0.1}_{-0.1}$

$^{\alpha}$ The powerlaw photon index of NTHCOMP. $^{\beta}$ Electron temperature of the Corona. $^{\gamma}$ Seed photon temperature of the disk.

$^{\delta}$ Normalisation of NTHCOMP. $^{\eta}$ Unabsorbed flux in the energy 4.0-16.0 keV for LAXPC 20 and 0.6-7.0 keV for SXT data.

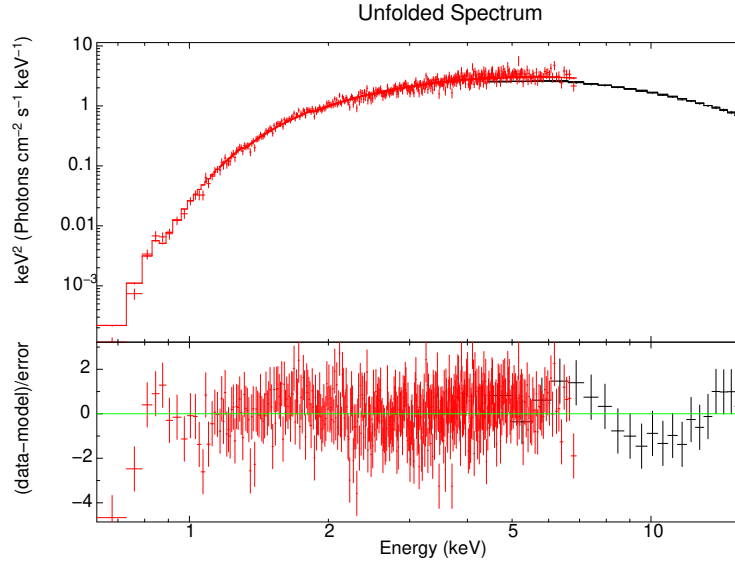


Figure 2.7: The unfolded spectra from *AstroSat* for GX 3+1 (SXT spectrum in red and LAXPC 20 layer 1 spectrum in black). The top panel shows the spectra fitted with the model Constant×TBABS×NTHCOMP. The energy band used is 0.6 - 16.0 keV. The bottom panel shows the ratio of data and model.

respectively), obtained using the convolution model CFLUX. These values are in agreement with the persistent flux reported by Pintore et al. (2015); Ludlam et al. (2019).

We have also attempted to add a DISKBB model to the NTHCOMP, but it has resulted in an overestimation of the errors in the fit. We have also tried to fit the pre-burst spectra by selecting the input type=0 so as to remodel the spectrum with blackbody seed photons. This has resulted in a poor fit, with a reduced chi-squared value rising to ~ 1.21 . However, adding a BBODY model to the NTHCOMP slightly lowered the reduced chi-squared value to ~ 1.18 , but the obtained

2. AstroSat observation of rapid Type-I thermonuclear burst from the low mass X-ray binary GX 3+1

normalization is found very small and its error limits couldn't be constrained.

2.4.2 Burst Analysis

We investigate the evolution of the free parameters during the dominant phase of the burst, by systematically dividing the burst exposure into a total of five time intervals- T1, T2, T3, T4 and T5, shown in Fig. 8. The exposure of the different time intervals are T1 = 0.8 s, T2 = 1.0 s, T3 = 0.9 s, T4 = 0.6 s and T5 = 2.4 s. We obtained the spectra for each of these five time bins from the top layer or layer 1 of the LAXPC 20. The energy band selected during XSPEC fitting is 4 - 16 keV. Harder energies more than 16 keV are ignored as the burst is observed predominantly present at softer energies (see Fig. 5). Energies lesser than 4.0 keV are ignored to avoid uncertainties in the response from LAXPC. As the model TBABS \times NTHCOMP has described the pre-burst spectra successfully, we proceed to investigate the burst by adding a blackbody model (Degenaar et al., 2016) BBODYRAD to pre-burst model (Galloway et al., 2008; Beri et al., 2016). The NTHCOMP is fed with pre-burst parameter values which are kept frozen and only the blackbody parameters are set free. This conventional approach is adopted to model all the five burst spectra, shown in Fig. 9. A systematic error of 2% is considered to account for the uncertainties in the spectral response of LAXPC following the works of Antia et al. (2017); Misra et al. (2017); Sreehari et al. (2019, 2020); Kashyap et al. (2022); Majumder et al. (2022).

The Table. 2.3 reports the blackbody temperature and the normalisation constant achieved during the fitting. We notice that the temperature kT_{bb} reaches a local minimum of 1.61 ± 0.08 keV corresponding to which the Norm_{bb} reaches the maximum value = $496.05^{+138.64}_{-106.98}$. During T5, which is the decay phase of the burst, the blackbody temperature rises again following a drop in the normalisation value. We could also observe that the unabsorbed flux is nearly constant from time bin T2 to T4 (the time interval during which the burst has shown the double peak at higher energies). We highlight that at T2, the Norm_{bb} is obtained with an almost six fold increase from T1. The normalisation values are used to estimate the radius using the relation⁷ $\text{Norm}_{\text{bb}} = R^2/D_{10\text{kpc}}^2$ and we achieve the maximum value of the photospheric radius $13.58^{+1.89}_{-1.46}$ km which agrees with the inner disk radius reported by Mondal et al. (2019) using *NuSTAR* data, in which they have also mentioned an upper limit of ≤ 13 km to the NS radius. To showcase all these parametric changes involved during the burst span, we have plotted the physical parameters vs time with t=0 as the burst rise in Fig. 10. We have not used any color correction factor to derive the radius and the burst temperature. The radii values are estimated for a source distance of 6.1 kpc (Kuulkers & van der Klis, 2000) reported for a helium rich photosphere.

⁷<https://heasarc.gsfc.nasa.gov/xanadu/xspec/manual/node137.html>

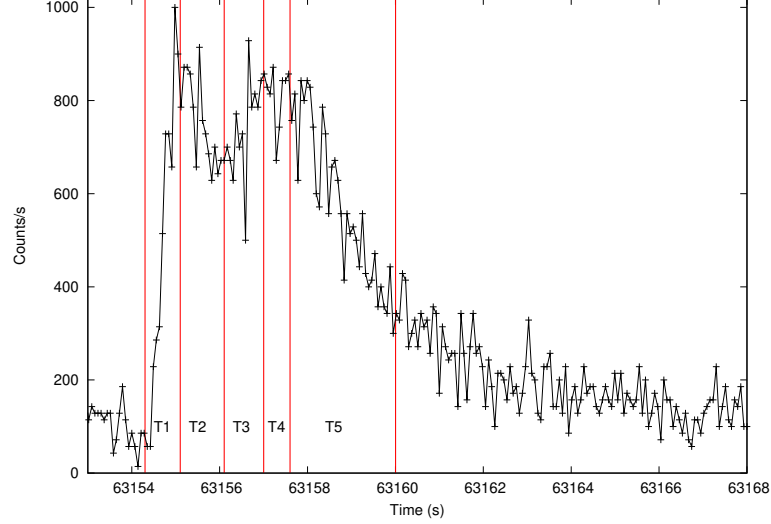


Figure 2.8: The time bins selected for spectroscopy. The burst light curve shown here is in 8-12 keV energy band.

Table 2.3: The best-fit parameters of BBODYRAD achieved during time resolved spectroscopy of the burst. The model fitted is TBABS \times (NTHCOMP + BBODYRAD). The parameter values of TBABS and NTHCOMP are kept frozen to the values achieved during modelling of the pre-burst emission. The energy band taken here for all the time bins is 4.0-16.0 keV. All the errors are at 90% confidence range

Parameter	T1	T2	T3	T4	T5
BBODYRAD					
kT_{bb}^{α}	$2.30^{+0.16}_{-0.14}$	$1.84^{+0.06}_{-0.06}$	$1.61^{+0.08}_{-0.08}$	$1.83^{+0.07}_{-0.07}$	$2.0^{+0.06}_{-0.06}$
$Norm_{bb}^{\beta}$	$46.82^{+14.13}_{-11.10}$	$269.42^{+44.8}_{-38.3}$	$496.05^{+138.64}_{-106.98}$	$301.40^{+60.7}_{-50.51}$	$124.78^{+17.18}_{-15.09}$
Radius $^{\gamma}$	$4.16^{+0.60}_{-0.47}$	$9.43^{+0.88}_{-0.75}$	$13.58^{+1.89}_{-1.46}$	$10.6^{+1.06}_{-0.88}$	$6.81^{+0.46}_{-0.41}$
$\chi^2/d.o.f$	0.81	1.16	1.65	1.12	1.67
Flux $^{\delta}$	$1.12^{+0.15}_{-0.15}$	$2.58^{+0.24}_{-0.24}$	$2.54^{+0.23}_{-0.23}$	$2.76^{+0.26}_{-0.26}$	$1.67^{+0.1}_{-0.1}$

$^{\alpha}$ The blackbody temperature in keV units.

$^{\beta}$ Normalisation constant of BBODYRAD in given by $Norm_{bb} = R^2/D_{10kpc}^2$, where R is the radius in km and D_{10kpc}^2 is the source distance in units of 10 kpc.

$^{\gamma}$ Radius of the photosphere in units of km, estimated for a source distance of 6.1 kpc.

$^{\delta}$ Unabsorbed blackbody flux in 10^{-8} ergs s^{-1} cm^{-2} units.

2.5 Discussions

In this work, we report the *AstroSat* observation of the bright atoll source, the LMXB GX 3+1. The light curve obtained from LAXPC 20 instrument indicated the presence of a thermonuclear burst feature of Type-1. Our temporal analysis revealed that the instrument SXT had observed the source simultaneously with the LAXPC 20 during the pre-burst stage till ~ 2 minutes before the burst was detected by LAXPC 20. Since LAXPC is operational during both orbital day

2. *AstroSat* observation of rapid Type-I thermonuclear burst from the low mass X-ray binary *GX 3+1*

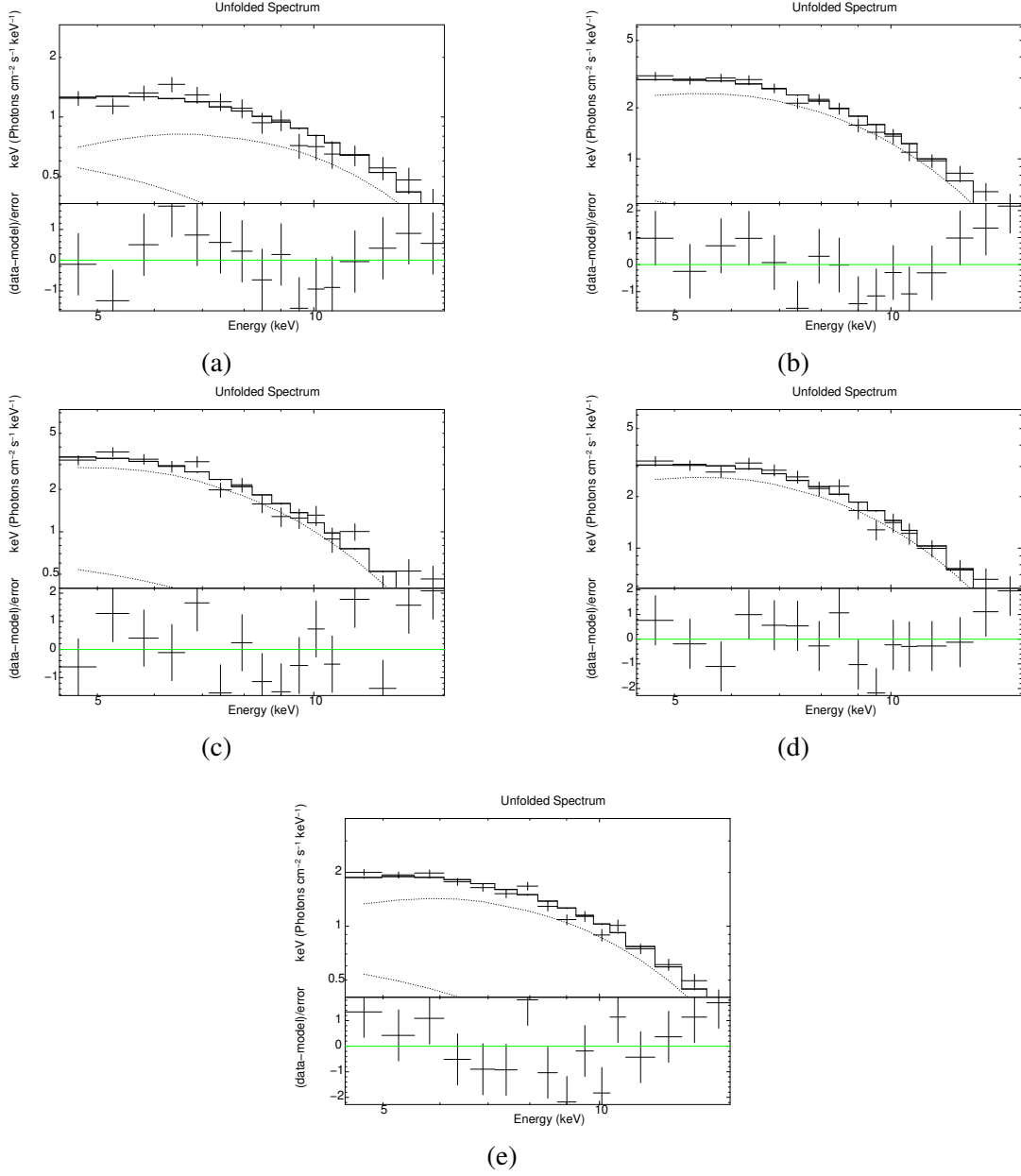


Figure 2.9: Time resolved spectroscopy of the burst using 5 time bins. We modelled the spectra during rise T1 shown by Fig.(a), Fig.(b), (c), (d) and (e) are the unfolded modelled spectra corresponding to the time bins T2, T3, T4, and T5. Each of the spectra is fitted following the conventional method on $TBABS \times (NTHCOMP + BBODYRAD)$. NTHCOMP parameters are frozen at pre-burst values for all the spectra.

and night and SXT can only observe during orbital night, there is more exposure by LAXPC than SXT prior to the satellite entering the South Atlantic Anomaly (SAA) passage. Hence, unfortunately, SXT data is not available during the thermonuclear burst.

It's noteworthy that the large collective area of LAXPC has allowed us to generate an energy resolved burst profile and we have followed Beri et al. (2019) and Bhulla et al. (2020). A drop in count rate in the light curve of the X-ray burst is observed when the narrow energy bands

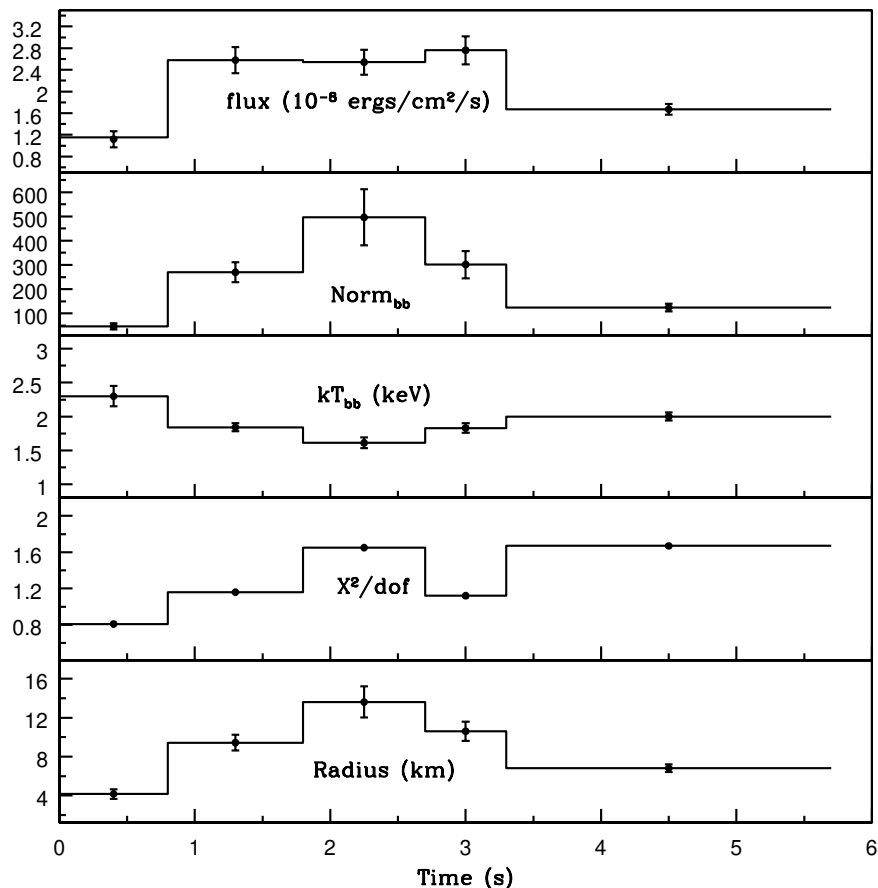


Figure 2.10: A combined plot of the evolution of unabsorbed flux, the normalisation constant of blackbody model, blackbody temperature kT_{bb} , the model error and the estimated photospheric radius in km for a source distance of 6.1 kpc. The x-axis counts the time from the rise of the burst.

become harder. Also, we found that the burst was brightest in 5-8 keV energy band with a count rate higher than the softest band 3-5 keV. From our QDP modelling, we find that the burst decays faster at higher energies, which indicates that the temperature is decreasing as the burst evolves. This trend is similar to the behaviour of the burst from 4U 1636-536, an atoll source, reported by Beri et al. (2019). We also noticed a double - peak feature in the burst at higher energies i.e 8-12 keV, 12-20 keV. This is a quick event ~ 2 s within which the burst had showed the double peak, indicating a radius expansion phase (Watts & Maurer, 2007; Paczynski, 1983). It is necessary to highlight that double peak bursts are also observed for bursts categorized as non-PRE bursts (Regev & Livio, 1984), where the double peak feature is observed for low energies as well, theoretically modelled by Fujimoto et al. (1988); Melia & Zylstra (1992); Fisker et al. (2004); Bhattacharyya & Strohmayer (2006); Zhang et al. (2009); Lampe et al. (2016) and Bult et al. (2019).

We now discuss about our modelling of the pre-burst or persistent spectra. The seed photon temperature is found to be < 1 keV in the literature reports of GX 3+1, but Pintore et al. (2015) has obtained values ≥ 1 keV for their two used models, both involving the thermally

2. *AstroSat* observation of rapid Type-I thermonuclear burst from the low mass X-ray binary GX 3+1

Comptonized NTHCOMP without fixing the seed photon temperature with the disk blackbody temperature. In our case the persistent pre-burst spectrum is fitted by an NTHCOMP for a disk blackbody emission and without any explicit DISKBB (Mitsuda et al., 1984; Makishima et al., 1983). The kT_{nth} is obtained to be > 1.8 keV. This is in close agreement to inner disk temperature reported by Mondal et al. (2019). We mention that the atoll source 4U 1728-34 is reported with seed photons > 1.6 keV by Bhattacharyya et al. (2018) for an NTHCOMP model with disk blackbody as input (no explicit disk blackbody component is used). We also mention that we could not improve the fitting of the pre-burst spectra by adding DISKBB or BBODY models to NTHCOMP. Since we have used the NTHCOMP model only to model the pre-burst spectrum where blackbody seed photons were not the input, the Comptonizing layer must have primarily covered the disk (Bhattacharyya et al., 2018).

During the spectral modelling of the burst, we have used the model BBODYRAD which directly leads to estimate the radius of the source. We find that the photosphere shrinks and the radius reaches to a value ~ 6.81 km during the decay of the burst. Bhattacharyya et al. (2018) systematically examined the relative differences in the blackbody normalization value achieved for both the conventional and the " f_a " method, and the latter has been found to provide lower normalisation values and hence a smaller NS radius. We have also tried adopting the f_a methodology to model burst spectra, but the data quality is not good enough to constrain complex models. Referring to Fig. 10, we see that the photospheric radius increases and reaches a local maximum at the same time when the blackbody temperature kT_{bb} reaches the minimum value as it could be seen at the top plot. From T2 to almost T4, which describes the PRE episode, the unabsorbed X-ray flux is found to remain approximately constant at $\sim (2.58-2.76 \text{ in } 10^{-8} \text{ ergs s}^{-1} \text{ cm}^{-2})$, which is expected for a PRE burst (Strohmayer & Bildsten, 2006; Galloway et al., 2008). During the double-peak event the source contracts and the photosphere expands thus the flux and hence the luminosity is expected to remain almost constant. This is derived from the understanding that luminosity is directly dependent to both the source temperature and the radius. The expansion of the photosphere leads to a drop in photon temperature and thus X-ray count rate drops (Tawara et al., 1984). Studies performed using the BeppoSAX data by Beri et al. (2016) indicated the presence of high temperatures (~ 3 keV) for X-ray bursts showing double-peaked profiles at higher energies, however, we don't find the presence of such high temperatures during the touchdown period. Since we have used a frozen pre-burst model as a background to the burst spectra, hence we are unable to investigate the effect of burst on the persistent emissions during the PRE event which was previously carried out for a non-PRE burst by Bhattacharyya et al. (2018).

It is worthy to mention that during the years 1983-2006, most of the reports of bursts from GX 3+1 had been published after which no burst event is reported for almost more than a decade. As mentioned in our Introduction (Sec. 1.), the first measurement of the radius of the NS was carried out by Kuulkers & van der Klis (2000) and the authors have reported a radius of be 4.5 ± 0.3 km during the non-burst period. This is consistent with the radius value derived by us

during T1 (rise of the burst, see Fig. 10) $\sim 4.16 \pm 0.53$ km. A single blackbody approximation on burst spectrum modelled by Molkov et al. (1999) had reported the NS radius to be 7.2 ± 1.2 km for a considered source distance of 8.5 kpc. If we consider a source distance of 8.5 kpc, we obtain the touchdown radius to be ~ 9.5 km. To add, the estimation of source distance could be well derived during a PRE, and ever since Kuulkers & van der Klis (2000) had reported it, the source distance hasn't been calculated with a greater precision. Since we could detect a PRE event, we attempt to estimate the source distance. The peak luminosity during the PRE event is considered to reach the source's Eddington luminosity, as the NS surface is lifted up. We use this opportunity to estimate the source distance by using the peak flux obtained by us, from Table. 3. The peak photon flux (F_b) is related to the Eddington luminosity (L_{Edd}) by a linear equation, which is the modified Stefan-Boltzmann law for an LMXB, given by Lewin et al. (1993):

$$L_{\text{Edd}} = 4\pi d^2 \xi_b F_b \quad (2.1)$$

Here, we have assumed the anisotropy constant ξ_b to be unity, which corresponds to the isotropic case. The subscript 'b' stands for burst. Keeping this equation in mind, we proceed towards deriving the Eddington luminosity from the equation (Pike et al., 2021)

$$L_{\text{Edd}} = \frac{4\pi cGM}{\kappa_0} \left[1 - \frac{2GM}{c^2 R} \right]^{1/2} \times \left[1 + \left(\frac{kT}{39.2 \text{ keV}} \right)^{0.86} \right] (1 + X)^{-1} \quad (2.2)$$

where M is the mass of the NS, G is the gravitational constant and c is the speed of light. We have assumed a typical NS mass of $1.4 M_{\odot}$. We have considered the hydrogen mass fraction $X=0$ and the typical upper limit of the NS radius as $R = 10$ km. We use the value of $\kappa_0 = 0.2 \text{ cm}^2 \text{ g}^{-1}$, which is the opacity factor for pure He (Pike et al., 2021). Using the value of kT_{bb} for the T4 time bin of Table. 3, we find the value of Eddington luminosity $L_{\text{Edd}} = 2.87 \times 10^{38} \text{ erg s}^{-1}$. Substituting this value of luminosity and choosing the value of F_b as the highest flux value from Table. 3, which corresponds to the T4 time bin in Eq. (2.1), we achieve the distance $d = 9.3 \pm 0.4$ kpc. For a range $0.5 < \xi_b < 2$ (Kuulkers & van der Klis, 2000), we obtain d in the range 6.6 - 13.2 kpc. We believe that to obtain source's physical parameters with greater accuracy, a refinement in the spectral analysis is required on a better data.

Acknowledgements

This report work has utilized the softwares provided by the High Energy Astrophysics Science Archive Research Centre (HEASARC). The authors AN and BS acknowledge the financial support of ISRO under *AstroSat* archival Data utilization program (No.DS_2B-13013(2)/2/2019-Sec.2). This publication uses data from the *AstroSat* mission of the Indian Space research Organization (ISRO), archived at the Indian Space Science Data Centre (ISSDC). AN acknowledges the Inter-University Center for Astronomy and Astrophysics (IUCAA), Pune for the periodic visits, the hospitality and the facilities provided to him to make possible the major part

2. AstroSat observation of rapid Type-I thermonuclear burst from the low mass X-ray binary GX 3+1

of the work. This work has been performed utilizing the calibration data-bases and auxiliary analysis tools developed, maintained and distributed by AstroSat-SXT team with members from various institutions in India and abroad. This research has made use of MAXI data provided by RIKEN, JAXA and the MAXI team (Matsuoka et al., 2009). BS also acknowledges the visiting associateship program at IUCAA and is grateful to IUCAA for hospitality during his visits where part of this work was done. AN thanks Dr. M. Pahari, Royal Society SERB International fellow for his useful suggestions in this work. AN personally thanks the scholar mates from Jamia Millia Islamia University, Delhi and other fellow mates who helped him resolve issues faced in this work. BS would like to acknowledge discussions held with Dr. Anjali Rao during the initial stages of this work. Authors are also indebted to the reviewer for providing beneficial suggestions and constructive comments, which has greatly enhanced the quality of the work.

Bibliography

- Alizai, K., Chenevez, J., Brandt, S., *et al.* 2020, MNRAS, 494, 2509
- Antia, H. M., Yadav, J. S., Agrawal, P. C., *et al.* 2017, ApJS, 231, 10.
- Antia, H. M., Agrawal, P. C., Dedhia, D., *et al.* 2021, Journal of Astrophysics and Astronomy, 42, 32.
- Arnaud, K. A. 1996, Astronomical Data Analysis Software and Systems V, 101, 17
- Asai, K., Dotani, T., Nagase, F., *et al.* 1993, PASJ, 45, 801
- Beri, A., Paul, B., Orlandini, M., *et al.* 2016, New Ast., 45, 48. doi:10.1016/j.newast.2015.10.013
- Beri, A., Paul, B., Yadav, J. S., *et al.* 2019, MNRAS, 482, 4397
- Belian, R. D., Connor, J. P., & Evans, W. D. 1976, IAU Circ., 2969
- Bhattacharya, D. & van den Heuvel, E. P. J. 1991, PhR, 203, 1
- Bhattacharyya, S. & Strohmayer, T. E. 2006, ApJL, 636, L121
- Bhattacharyya, S. 2010, Advances in Space Research, 45, 949
- Bhattacharyya, S. 2011, Astronomical Society of India Conference Series, 3, 15
- Bhattacharyya, S., Yadav, J. S., Sridhar, N., *et al.* 2018, ApJ, 860, 88.
- Bhattacharyya, S., Singh, K. P., Stewart, G., *et al.* 2021, Journal of Astrophysics and Astronomy, 42, 17.
- Bhulla, Y., Roy, J., & Jaaffrey, S. N. A. 2020, Research in Astronomy and Astrophysics, 20, 098
- Bildsten, L. 2000, in AIP Conf. Proc. 522. Cosmic Explosions: Tenth Astrophysics Conference., ed. S. Holt, & W. Zhang (Melville: AIP), AIP Conf. Proc., 522, 359

Bibliography

- Bowyer, S., Byram, E. T., Chubb, T. A., *et al.* 1965, *Annales d'Astrophysique*, 28, 791
- Bradt, H. V., Rothschild, R. E., & Swank, J. H. 1993, *A&AS*, 97, 355
- Bult, P., Jaisawal, G. K., Güver, T., *et al.* 2019, *ApJL*, 885, L1.
- Chen, Y.-P., Zhang, S., Zhang, S.-N., *et al.* 2012, *ApJL*, 752, L34
- Chen, Y. P., Zhang, S., Zhang, S. N., *et al.* 2019, *Journal of High Energy Astrophysics*, 24, 23
- Chenevez, J., Falanga, M., Brandt, S., *et al.* 2006, *A&A*, 449, L5
- Degenaar, N., Ballantyne, D. R., Belloni, T., *et al.* 2018, *Space Sci. Rev.*, 214, 15
- Degenaar, N., Koljonen, K. I. I., Chakrabarty, D., *et al.* 2016, *MNRAS*, 456, 4256
- den Hartog, P. R., in't Zand, J. J. M., Kuulkers, E., *et al.* 2003, *A&A*, 400, 633
- Devasia, J., Raman, G., & Paul, B. 2021, *New Astron.*, 83, 101479
- Fisker, J. L., Thielemann, F.-K., & Wiescher, M. 2004, *ApJL*, 608, L61
- Fujimoto, M. Y., Sztajno, M., Lewin, W. H. G., *et al.* 1988, *A&A*, 199, L9
- Galloway, D. K., Munro, M. P., Hartman, J. M., *et al.* 2008, *ApJS*, 179
- Galloway, D. K., in't Zand, J., Chenevez, J., *et al.* 2020, *ApJS*, 249, 32.
- Grindlay, J., Gursky, H., Schnopper, H., *et al.* 1976, *ApJL*, 205, L127
- Homan, J., van der Klis, M., Wijnands, R., *et al.* 1998, *ApJL*, 499, L41
- Hoffman, J. A., Lewin, W. H. G., & Doty, J. 1977, *ApJL*, 217, L23
- Hoffman, J. A., Marshall, H. L., & Lewin, W. H. G. 1978, *Nature*, 271, 630
- Hu, C.-P., Begiçarslan, B., Güver, T., *et al.* 2020, *ApJ*, 902.
- in't Zand, J. J. M., Galloway, D. K., Marshall, H. L., *et al.* 2013, *A&A*, 553, A83
- Kashyap, U., Chakraborty, M., & Bhattacharyya, S. 2022, *MNRAS*, 512, 6180.
- Kashyap, U., Ram, B., Güver, T., *et al.* 2022, *MNRAS*, 509, 3989
- Kubota, A., Makishima, K., & Ebisawa, K. 2001, *ApJL*, 560, L147
- Keek, L., Arzoumanian, Z., Bult, P., *et al.* 2018, *ApJL*, 855, L4
- Kuulkers, E. & van der Klis, M. 2000, *A&A*, 356, L45
- Kuulkers, E. 2002, *A&A*, 383, L5

- Lampe, N., Heger, A., & Galloway, D. K. 2016, ApJ, 819, 46.
- Levine, A. M., Bradt, H., Cui, W., *et al.* 1996, ApJL, 469, L33
- Lewin, W. H. G., van Paradijs, J., & Taam, R. E. 1993, Space Sci. Rev, 62, 223.
- Ludlam, R. M., Miller, J. M., Barret, D., *et al.* 2019, ApJ, 873, 99
- Majumder, S., Sreehari, H., Aftab, N., *et al.* 2022, MNRAS, 512, 2508.
- Makishima, K., Mitsuda, K., Inoue, H., *et al.* 1983, ApJ, 267, 310
- Makishima, K., Maejima, Y., Mitsuda, K., *et al.* 1986, ApJ, 308, 635
- Maqbool, B., Mudambi, S. P., Misra, R., *et al.* 2019, MNRAS, 486, 2964
- Marino, A., Del Santo, M., Cocchi, M., *et al.* 2019, MNRAS, 490, 2300.
- Matsuoka, M., Kawasaki, K., Ueno, S., *et al.* 2009, PASJ, 61, 999
- Melia, F. & Zylstra, G.~J. 1992, ApJL, 398, L53.
- Misra, R., Yadav, J. S., Verdhhan Chauhan, J., *et al.* 2017, ApJ, 835, 195.
- Mitsuda, K., Inoue, H., Koyama, K., *et al.* 1984, PASJ, 36, 741
- Molkov, S. V., Grebenev, S. A., Pavlinsky, M. N., *et al.* 1999, Astrophysical Letters and Communications, 38, 141
- Mondal, A. S., Dewangan, G. C., & Raychaudhuri, B. 2019, MNRAS, 487, 5441
- Morrison, R. & McCammon, D. 1983, ApJ, 270, 119
- Mudambi, S. P., Maqbool, B., Misra, R., *et al.* 2020, ApJL, 889, L17
- Oosterbroek, T., Barret, D., Guainazzi, M., *et al.* 2001, A&A, 366, 138
- Paczynski, B. 1983, ApJ, 267, 315
- Paizis, A., Farinelli, R., Titarchuk, L., *et al.* 2006, A&A, 459, 187
- Pavlinsky, M. N., Grebenev, S. A., & Sunyaev, R. A. 1994, ApJ, 425, 110.
- Pike, S. N., Harrison, F. A., Tomsick, J. A., *et al.* 2021, ApJ, 918, 9
- Pintore, F., Di Salvo, T., Bozzo, E., *et al.* 2015, MNRAS, 450, 2016
- Piraino, S., Santangelo, A., Kaaret, P., *et al.* 2012, A&A, 542, L27
- Regev, O. & Livio, M. 1984, A&A, 134, 123

Bibliography

- Roy, P., Beri, A., & Bhattacharyya, S. 2021, MNRAS, 508, 2123
- Schulz, N. S., Hasinger, G., & Truemper, J. 1989, A&A, 225, 48
- Seifina, E. & Titarchuk, L. 2012, ApJ, 747, 99
- Singh, K. P., Stewart, G. C., Chandra, S., *et al.* 2016, Proc. SPIE, 9905, 99051E
- Singh, K. P., Stewart, G. C., Westergaard, N. J., *et al.* 2017, Journal of Astrophysics and Astronomy, 38, 29
- Sreehari, H., Ravishankar, B. T., Iyer, N., *et al.* 2019, MNRAS, 487, 928.
- Sreehari, H., Nandi, A., Das, S., *et al.* 2020, MNRAS, 499, 5891.
- Strohmayer, T. & Bildsten, L. 2006, Compact stellar X-ray sources, 113
- Strohmayer, T. E., Altamirano, D., Arzoumanian, Z., *et al.* 2019, ApJL, 878, L27
- Swank, J. H., Becker, R. H., Boldt, E. A., *et al.* 1977, ApJL, 212, L73.
- Tawara, Y., Kii, T., Hayakawa, S., *et al.* 1984, ApJL, 276, L41.
- van den Berg, M., Homan, J., Fridriksson, J. K., *et al.* 2014, ApJ, 793, 128
- Verdhan Chauhan, J., Yadav, J. S., Misra, R., *et al.* 2017, ApJ, 841, 41
- Verbunt, F. 1993, ARAA, 31, 93
- Watts, A. L. & Maurer, I. 2007, A&A, 467, L33
- Wilms, J., Allen, A., & McCray, R. 2000, ApJ, 542, 914
- Worpel, H., Galloway, D. K., & Price, D. J. 2013, ApJ, 772, 94
- Worpel, H., Galloway, D. K., & Price, D. J. 2015, ApJ, 801, 60
- Yadav, J. S., Misra, R., Verdhan Chauhan, J., *et al.* 2016, ApJ, 833, 27
- Zdziarski, A. A., Johnson, W. N., & Magdziarz, P. 1996, MNRAS, 283, 193
- Zhang, G., Méndez, M., Altamirano, D., *et al.* 2009, MNRAS, 398, 368.
- Życki, P. T., Done, C., & Smith, D. A. 1999, MNRAS, 309, 561

Chapter 3

Probing the accretion flow properties of NS LMXB 4U 1608-52 using AstroSat observations

Ankur Nath,¹ Biplob Sarkar,¹ Aru Beri² Ranjeev Misra³

¹Dept. of Applied Sciences, Tezpur University, Tezpur, Assam, India

²DST-INSPIRE Faculty, IISER Mohali, Punjab, India

³Inter-University Center for Astronomy and Astrophysics, Ganeshkhind, Pune

Abstract

The source 4U 1608-52 was observed for ~ 40 ks with LAXPC (Large Area X-ray Proportional Counters) instrument on board AstroSat. AstroSat observed this source when the source was descending to a period of quiescence, evident from the long-term Swift-BAT (15-50 keV) and MAXI (2-20 keV) light curves. This indicates that the source was in a hard-intermediate state during AstroSat's observation. A strong positive correlation between the photon's hardness ratio and the source's intensity is detected. Due to such variability, the flux-resolved spectroscopy is performed on source spectra extracted from the Soft X-ray Telescope (SXT) and LAXPC 10 and 20 counters. Our analysis shows that the photon index decreases from ~ 2.26 to ~ 1.85 , whereas the electron temperature stays approximately constant at ~ 2.9 keV. This indicates that further analysis is needed on 4U 1608-52 to understand its disk geometry better.

Keywords— X-rays: binaries—stars: neutron—pulsars: individual: 4U1608-52—X-rays: stars—methods: data analysis—AstroSat: LAXPC/SXT

3.1 Introduction

X-ray binary systems have strong gravitational centers, either compact neutron stars or black holes. Based on the lower mass of the companion stars ($< 3 M_{\odot}$), we have the Low Mass X-ray binaries (LMXBs) as a sub-category of binary systems. According to the pattern traced by LMXBs in their color-color diagram (CCD), which is a plot of the high energy X-ray photon ratio (hard color) vs. the low energy photon ratio (soft color), such sources are sub-divided into atoll and Z sources. 4U 1608-52 is an established atoll source LMXB (Hasinger & van der Klis, 1989; van Straaten, van der Klis, & Méndez, 2003) and like most of the LMXB's, this source is a transient source (Güver et al., 2010) with a neutron star (NS) at its center (Tananbaum et al., 1976). Some of the earlier literature reports of 4U 1608-52, such as Gierliński & Done (2002); van Straaten, van der Klis, & Méndez (2003); Chen, Zhang, & Ding (2006); Kajava et al. (2017) with Rossi X-ray Timing Explorer (RXTE), Chen et al. (2019) with Insight-HXMT observation, involve extensive study of its extracted spectra and mapping of its recorded timing properties. This source has always shown frequent outbursts (Gierliński & Done, 2002; Zhang et al., 1996) with a shorter quiescence period (Šimon, 2004; Chen, Shrader, & Livio, 1997).

The atoll type LMXBs shows spectral variability, which is well displayed in the plot of the Hardness ratio (ratio of high energy X-ray photons and soft energy photons) vs. the source intensity, and two distinct states are identified from the track the hardness ratio follows - the banana and the island state. Banana states are marked as the soft states with a positive or almost no variability in the photon hardness for a wide range of intensity, whereas island states are identified as the harder states at lower intensities. In banana states, higher luminosities with soft spectra are observed (Di Salvo et al., 2000; Piraino, Santangelo, & Kaaret, 2000). Atoll sources move along the banana track as it goes from lower to higher luminosity; thus, the lower and upper banana states are classified. Although the photon hardness mapping helps understand the spectral changes, the correlations observed in such mapping can be better studied and parametrized by spectral modeling of the source.

The spectra of LMXBs are reported to be successful with two-component modeling - a thermal power-law plus a softer blackbody component. Two of the widely accepted model types are (1). the Eastern Model (Mitsuda et al., 1984, 1989) assumes a softer component from the disk, and (2). the Western Model (White, Stella, & Parmar, 1988), where the softer component is characterized as a surface emission. The Comptonised harder component is assumed to result from corona or boundary emission/inner disk in both models (Falanga et al., 2006; Paizis et al., 2006). Chen, Zhang, & Ding (2006) modeled 4U 1608-52 with Comptonized cutoff power-law plus a blackbody. Chen et al. (2019) used a thermal Comptonised power-law added to a blackbody, and they claimed to fit the spectra with a multi-colored blackbody emission from the disk - the disk blackbody Mitsuda et al. (1984). Besides considering such models, the accretion physics also demands the inner disk region to be illuminated by the boundary layer (Gierliński & Done, 2002), which are identified as broad iron line emissions ($\sim 6-7$ keV). These

are modeled with Gaussian models (Chen, Zhang, & Ding, 2006). The first iron-line emissions from 4U 1608-52 were reported by Suzuki et al. (1984). Also, Yu et al. (1997) had reported kHz quasi-periodic oscillations from 4U 1608-52 for the first time, with *RXTE/PCA*. Yu et al. (1997) report was during an observation performed on this source, at its decaying phase from an outburst (Marshall & Angelini, 1996). Now, we have mentioned the variability of photon hardness ratio with the flux intensity of LMXBs, and to analyze the spectra in such cases, single modeling of the entire spectra overlooks the parametric changes during the evolution of the hardness. So instead of a single spectrum of long exposure, we take several spectra generated at their respective flux states. The spectra are modeled individually, and the variations in parameters like the electron temperature of the corona, and the photon index directly obtained by THCOMP (Zdziarski et al., 2020), in XSPEC, are monitored. Changes in these parameters directly indicate the corresponding variation in the physical features of the boundary layer and the corona. A study based on various source literature shows that it is expected for the photon index to show a monotonic anti-correlation with the corona temperature (Farinelli & Titarchuk, 2011). The heating of the corona immediately steepens the spectra, which is well-described by the lowering of the photon index. The reverse effect has also been found, where the source descends to softer spectra with a lowering of electron temperature with the flux (Falanga et al., 2006); however, Falanga et al. (2006) could not show the increase in photon index as they expected.

We now discuss *Astrosat*, the first Indian multi-wavelength space observatory. Large Area Proportional Counters (LAXPC) with its three units - LAXPC 10, 20, and 30 and Soft X-ray Telescope (SXT), are the two instruments on board *Astrosat* dedicated to X-ray astronomy. SXT operates in the energy band 0.3-8.0 keV, whereas the LAXPC counters are built to operate in a broad energy band, from 3.0 keV to a maximum of 80.0 keV. *AstroSat* has observed various LMXBs, and the data have been spectrally modeled by Bhulla, Roy, & Jaaffrey (2020) and Beri et al. (2019) using a soft blackbody in addition to a thermal Comptonized component. However, Agrawal et al. (2018) was successful in modeling the spectra of LMXB 4U 1705-44, using a thermal Comptonised model added to a non-thermal power law, which has been modified further by a Gaussian. Report of the Z type LMXB LMC X-2 by Agrawal & Misra (2009) using *RXTE* data shows the use of a multi-color disk blackbody added to a single Comptonisation component. Agrawal & Nandi (2020) modeled the spectra of this same source with a combination of a disk blackbody model and a black body.

In this chapter, we report the X-ray data analysis of LMXB 4U 1608-52 using *AstroSat* mission data for the first time. We discuss the data reduction procedures obtained and report the detailed temporal behavior in section 3.2. We have followed a spectral analysis based on the source's flux intensity. We report the parametric values obtained in section 3.4 and discuss our observations with previously reported source parameters in section 3.5.

3. Probing the accretion flow properties of NS LMXB 4U 1608-52 using *AstroSat* observations

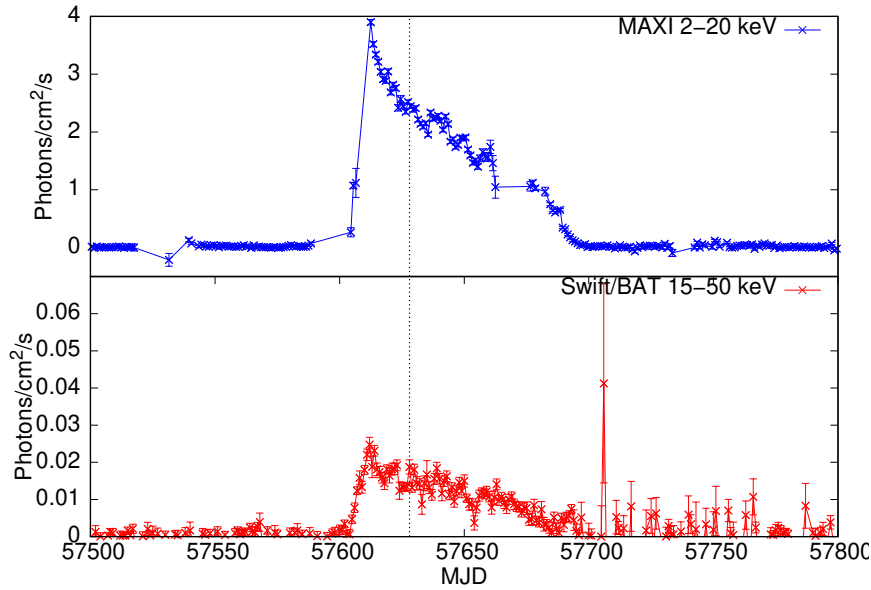


Figure 3.1: The observation by *AstroSat* is marked with the black dotted line on MAXI (upper panel) and Swift/BAT (lower panel) daily light curves. *AstroSat* could capture it during its descent from an outburst

3.2 Data reduction and Temporal Analysis

The source 4U 1608-52 was observed at 28th of August, 2016 for an exposure time- period ~ 40 ks by LAXPC (Obs.ID: G05_140T01_9000000628). The long term light curve from *SWIFT*/Burst Alert Telescope (BAT) and the Monitor of All-sky X-ray Image (MAXI) soft energy band light curve marks the *AstroSat* observation during a quick decay phase of the source from an outburst, as evident from Fig. 3.1.

We downloaded the level 1 version of SXT and LAXPC archive data from the official ISSDC website¹. For the temporal analysis, we collected the level 2 version of only LAXPC data, from the top layers of proportional counters 10 and 20 in Event Analysis mode (EA). We used response files while extracting the event file which are generated by the individual laxpc routine LAXPCSoft². All the light curves used have their background photons subtracted.

We have used the SXT spectrum later in this chapter, and we mention below the data reduction procedure undertaken for this instrument. We have used the SXT pipeline version AS1SXTLevel2-1.4b, to generate the individual orbit level 2 data in Photon Count (PC) mode. A total of 8 orbit level 2 data is then merged together to generate a single event file, for which we have used the latest module supplied by the SXT team³ with a Julia based event merger tool, which uses a Julia version 1.0.5.

¹https://webapps.issdc.gov.in/astro_archive

²<http://astrosat-ssc.iucaa.in/laxpcData>

³<http://astrosat-ssc.iucaa.in/sxtData>

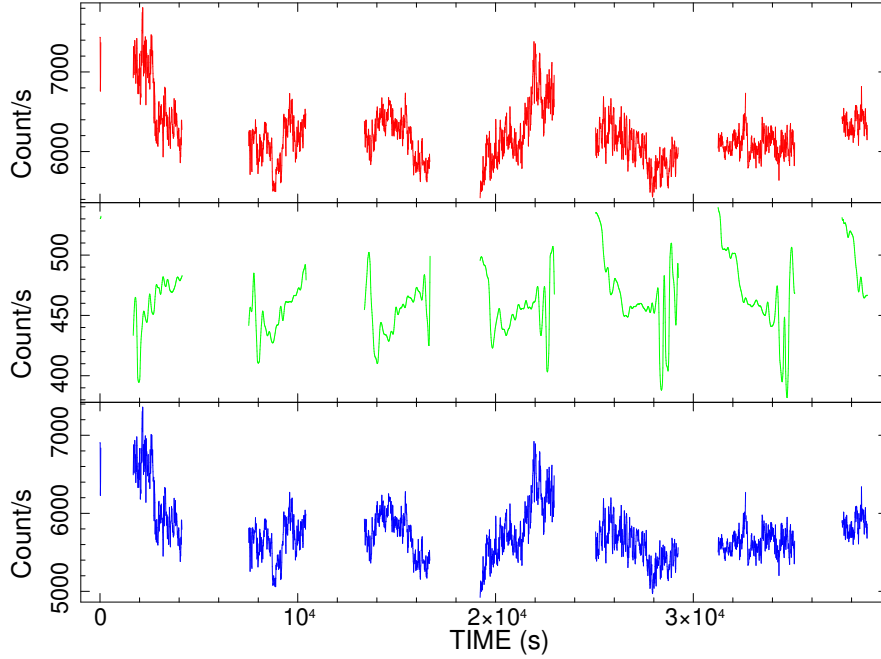


Figure 3.2: The light curve generated out of the total exposure data from laxpc 10 and 20 counters for a net energy range 3.0-80.0 keV (red), the background light curve of the same (green) and the final background subtracted light curve (blue). A binning time of 10 s is taken for all of the light curves.

3.2.1 Light curve

We first checked the long exposure light curve only for the Good Time Intervals (GTI), with a binning of 10.0 s, in the entire permissible energy band of 3.0-80 keV, using LAXPC 10 and 20. The background count rate is found quite lower with respect to the source, which is evident from almost no difference seen in the light curve, after we have subtracted the background photons, see Fig. 3.2. We didn't notice any rapid burst feature in our observation, but the net count rate is found irregular.

The SXT light curve (Fig. 3.3) is generated for a binning of 2.3775 s which is the smallest allowed binning of SXT. Initially, we observed that SXT light curve is hugely piled up, with its count rate reaching ~ 116 c/s. In order to cope with this massive pile up, we have crop out an annular region of 6 arcmins and 12 arcmins of inner and outer radii, respectively. This region filter could attain an acceptable SXT average count rate of 28.60 c/s, which is lower than the upper limit advisable, set by the SXT team for pile-up cases. The annular region chosen was based on a radial profile check on 4U 1608-52, which is performed by SAOImage DS9 version 7.4.

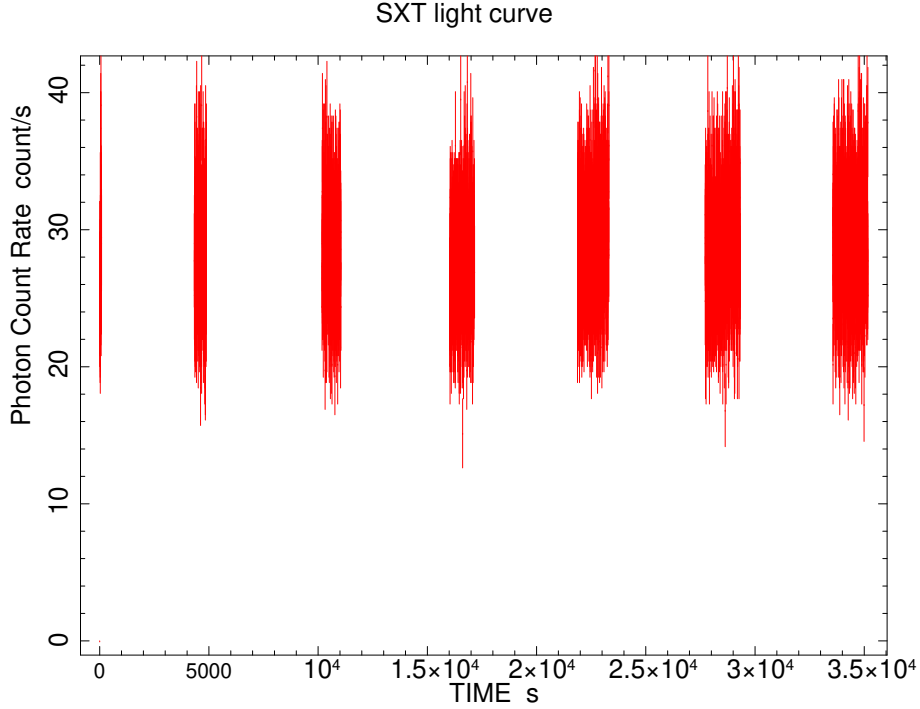


Figure 3.3: The SXT light curve is shown here for an energy range 0.3-8.0 keV (red), A binning time of 2.3775 s is taken.

3.2.2 Color-Color and Hardness analysis

To have a preliminary idea of what spectral changes the sources could have possibly gone through, we generated the Color-Color diagram (CCD) and the Hardness plots. Background light curves are generated for each of the lightcurves used and to eliminate the mapping of background photons, we subtracted them from the respective light curves, to generate Fig. 3.4, Fig. 3.5 and Fig. 3.6.

We have kept a soft-color ratio B/A and a hard color ratio C/B , where A, B, C are light curves in the energy bands 3.0-6.0 keV, 6.0-12.0 keV and 12.0-20.0 keV, respectively. see Fig. 3.4. The CCD reveals the low dominance of hard color over the soft color and the same behaviour is observed to correlate in the Hardness-Intensity diagram (HID), where the relative hardness of the source is mapped against the total intensity in 7.5-18.0 keV. We used the definition of Hardness Ratio (HR) as the ratio of number of photon counts in the energy bands 12.0-20.0 keV and 3.0-6.0 keV respectively, for a binning time of 40.0 s. We could easily notice a high correlation of HR with the intensity (Fig. 3.5). Such a high positive relation strongly indicates how the source has ascended to an upper banana state (Fig. 3.6). This variability of the HR led us to further investigate the spectral change patterns, via a flux-resolved spectroscopy in which the entire source flux is divided into four dominant flux states, details of which are in section 3.5.

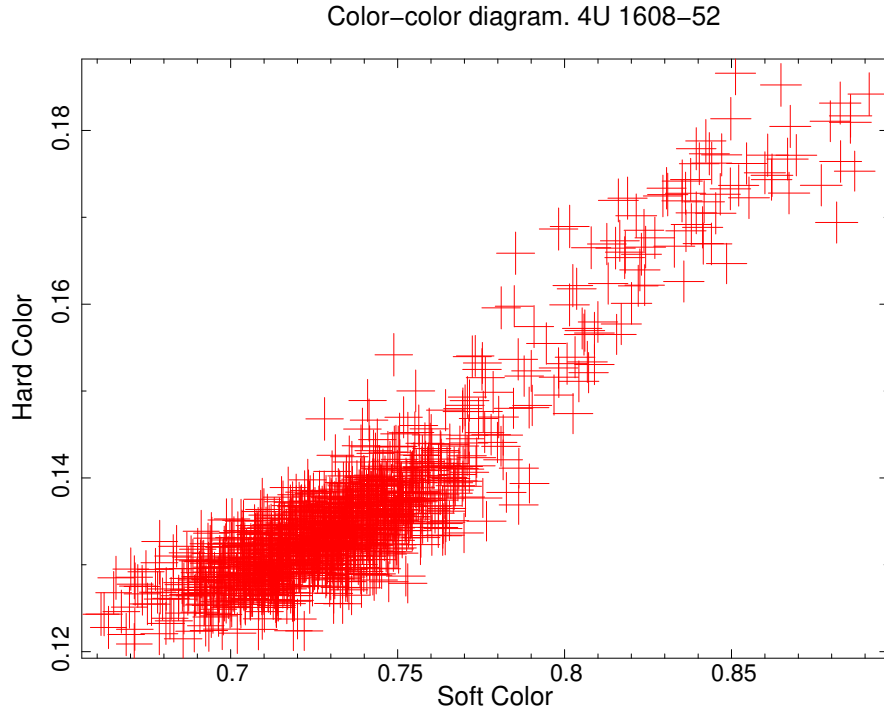


Figure 3.4: The Color Color Diagram of 4U 1608-52 with data from LAXPC 10 and 20 counters. 12.0 - 20.0 keV/6.0-12.0 is the Hard color ratio and 6.0-12.0/3.0-6.0 is the Soft color ratio.

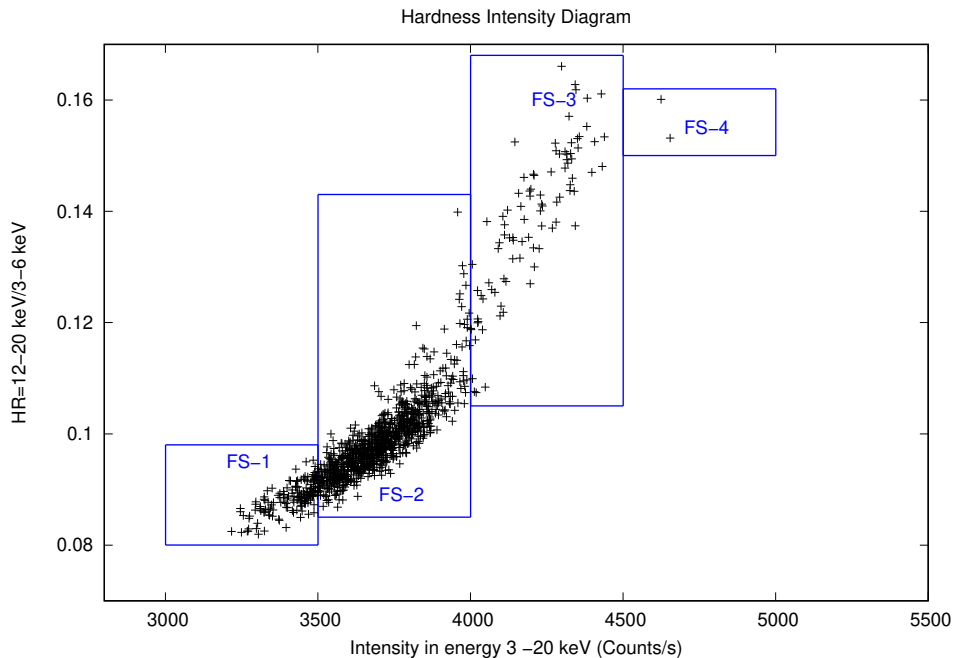


Figure 3.5: The Hardness Intensity Diagram using data from the top layer of LAXPC 10 and 20. We observe a strong positive correlation of Hardness ratio (HR) with the intensity. The entire flux is sub-divided into four flux states- FS-1, FS-2, FS-3 and FS-4 based on increasing intensity. Each of these flux states are spectrally analysed ahead to study the spectral evolution of the source with increasing flux.

3. Probing the accretion flow properties of NS LMXB 4U 1608-52 using AstroSat observations

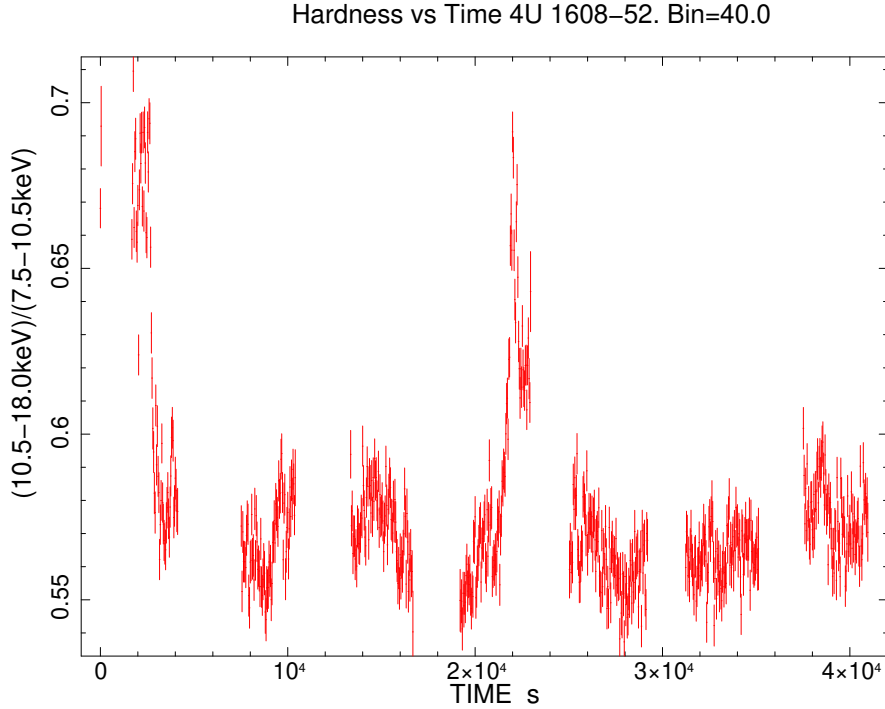


Figure 3.6: The evolution Hardness ratio of 4U 1608-52 with time.

Table 3.1: The PDS is fitted with a power law added to a lorentzian curve

PhoIndex	$1.96^{0.04}_{-0.04}$
$N_{\text{pow}}(\text{E-05})$	$3.44^{0.45}_{-0.43}$
lor Line E	$0.29^{0.06}_{-0.06}$
lor Width	$0.53^{0.06}_{-0.06}$
$\text{Norm}_{\text{lor}}(\text{E-04})$	$1.31^{0.31}_{-0.27}$
$\chi^2/d.o.f$	75.05/44

3.3 Timing analysis

Power density spectrum

The power density spectrum (PDS) is fitted with a powerlaw and a lorentzian and the photon index is found to be ~ 1.96 . The PDS is not modelled beyond 1.5 hz owing to high white noise. Features like quasi periodic oscillations (QPO) and pulsations are not found. The lorentzian line is found to be of intermediate width of 0.53 ± 0.06 . The powerlaw is found to contribute more at lower frequencies.

Time lag and Root mean squared power

The time lag and fractional root mean squared power (rms) vs energy plot is generated by using the command `laxpc_find_frelag` and the corresponding lowest frequency l is varied from 0.01 to 0.03 hz, to get better results. We select $l = 0.03$ hz and the highest frequency $h = 10$ hz. We have initially analysed time lag and fractional rms at frequencies (hz), $f = 0.05, 0.06, 0.07, 0.08, 0.09,$

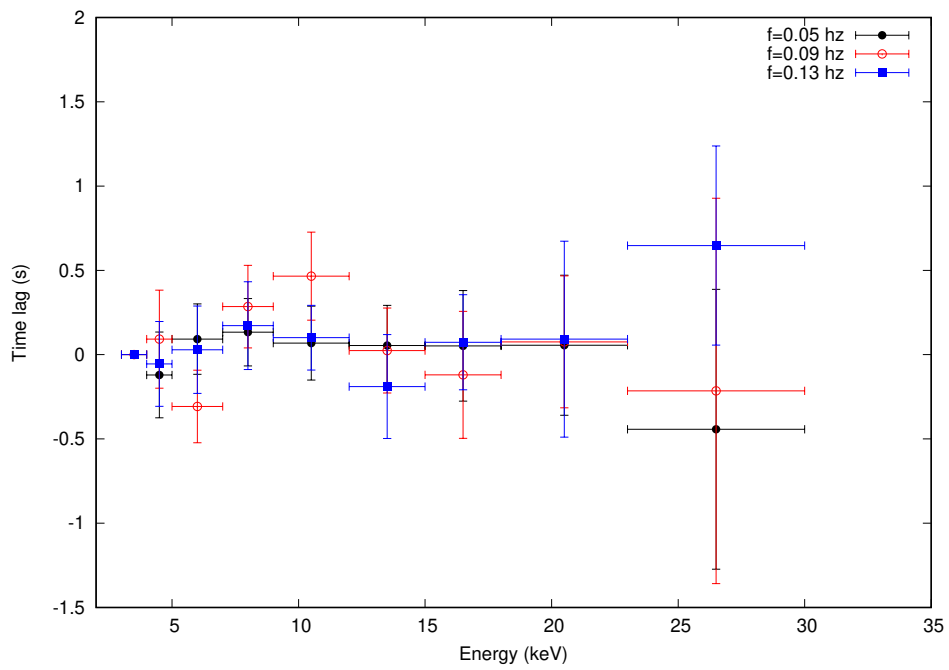
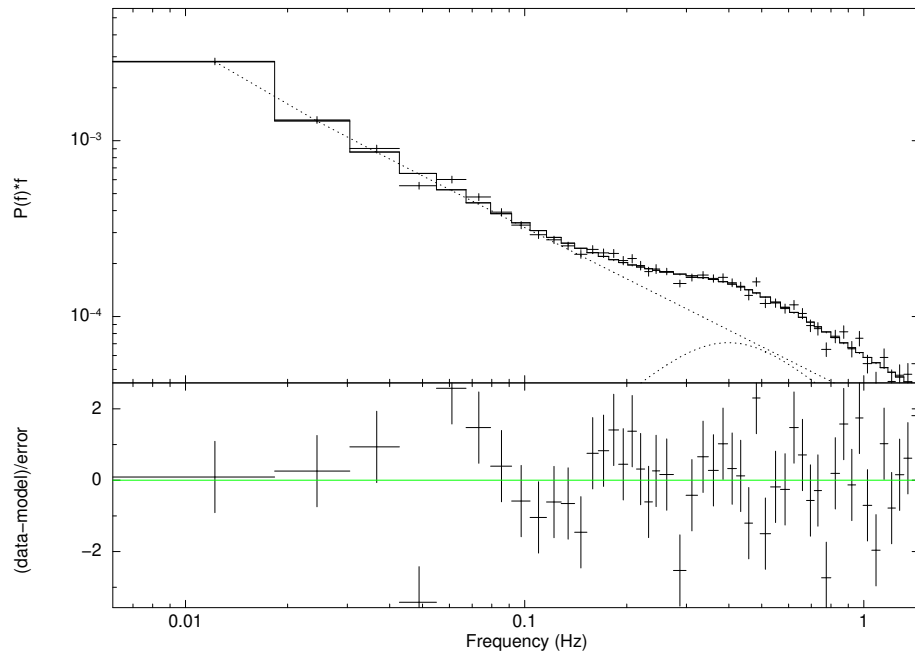


Figure 3.7: Time lag of photons vs energy in 3-35 keV

3. Probing the accretion flow properties of NS LMXB 4U 1608-52 using AstroSat observations

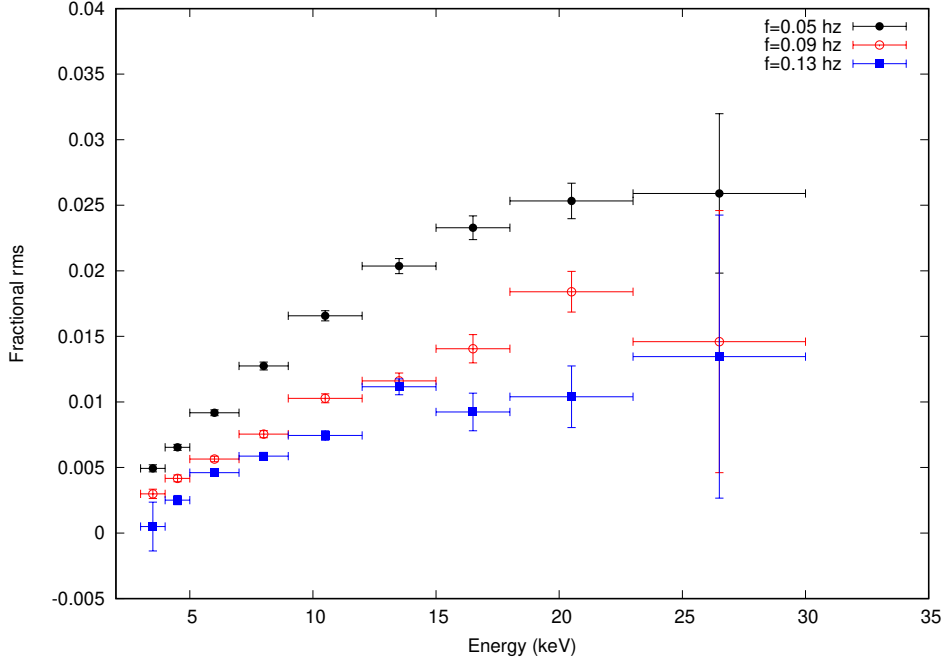


Figure 3.8: Fractional rms vs energy in 3-35 keV

0.1, 0.2, 0.3, 0.4, 0.5. Based on the plots, we selected three frequencies 0.05, 0.09 and 0.13 at which we have finally generated the time lag and fractional rms plot with respect to energy in keV.

The fractional rms is lower at softer energies and it rises upto 3% when, the curve doesn't show any further significant increase beyond 20 keV. The time lag of harder photons wrt to softer photons has been found to vary at different energies without any distinctive correlation. The time lag is found positive for frequency 0.13 Hz and negative for both 0.09 Hz and 0.05 Hz. Overall, we report that there is no significant time-lag of hard and soft photons. It is to mention that we have selected only LAXPC PCU 10 and 20 data for our timing analysis.

3.4 Flux resolved spectroscopy

Based on the source behaviour observed in the HID, we proceeded to investigate the source spectra through a flux-resolved spectroscopy- a modelling technique where each spectrum file is generated for a small flux range. Hence, we generated four Good Time Interval files for LAXPC counters 10 and 20 (GTI) by clipping off the light curve as per the following flux ranges- (1). 3000-3500 (Flux State 1 or FS-1) (2). 3500-4000 (FS-2) (3). 4000-4500 (FS-3) (4). 4500-5000 (FS-4) (see Fig. 3.6). Using these GTI files, spectra and the corresponding background spectra are generated for the top layer. We found that the background spectra is dominant over the source spectra, beyond ~ 20 keV, thus we exclude the spectral region higher than 20 keV while fitting. We also include here the data from the SXT instrument to analyse the soft energy spectra alongwith the LAXPC spectra. The spectra of SXT is obtained from the SXT light curve for the

Table 3.2: The best-fit parameter values for the joint spectral modelling of SXT, LAXPC 10 and LAXPC 20 layer 1 data using a model combination $\text{Constant} \times \text{TBABS} \times (\text{THCOMP} * \text{BBODY} + \text{GAUSS})$. Errors are at 90% confidence range for each parameter

Parameters	FS-1	FS-2	FS-3	FS-4
Const. LXP20	(1.0)	(1.0)	(1.0)	(1.0)
Const. LXP10	$0.95^{+0.01}_{-0.01}$	$0.96^{+0.13}_{-0.13}$	$0.96^{+0.13}_{-0.13}$	$0.96^{+0.01}_{-0.01}$
Const. SXT	$0.35^{+0.006}_{-0.006}$	$0.35^{+0.004}_{-0.004}$	$0.35^{+0.005}_{-0.005}$	$0.34^{+0.007}_{-0.007}$
Γ	$2.26^{+0.03}_{-0.03}$	$2.14^{+0.03}_{-0.03}$	$1.99^{+0.02}_{-0.02}$	$1.85^{+0.18}_{-0.18}$
kT_e (keV)	$2.93^{+0.07}_{-0.08}$	$2.90^{+0.06}_{-0.06}$	$2.90^{+0.05}_{-0.06}$	$2.92^{+0.05}_{-0.06}$
$\text{Line}_{\text{gauss}}$ (keV)	(6.4)	(6.4)	(6.4)	(6.4)
σ (keV)	$1.37^{+0.23}_{-0.23}$	$1.43^{+0.18}_{-0.18}$	$1.39^{+0.21}_{-0.21}$	$1.31^{+0.33}_{-0.31}$
N_{gauss} (E-02)	$5.55^{+0.01}_{-0.01}$	$7.82^{+0.01}_{-0.01}$	$7.94^{+0.01}_{-0.01}$	$5.63^{+0.02}_{-0.02}$
kT_{bb} (keV)	$0.58^{+0.02}_{-0.02}$	$0.58^{+0.01}_{-0.01}$	$0.54^{+0.02}_{-0.02}$	$0.48^{+0.02}_{-0.02}$
N_{bb}	(0.14)	(0.14)	(0.14)	(0.14)
N_{H} (10^{22} cm^{-2})	$1.05^{+0.06}_{-0.06}$	$1.05^{+0.04}_{-0.04}$	$1.11^{+0.06}_{-0.06}$	$1.18^{+0.08}_{-0.08}$
$\chi^2/\text{d.o.f}$	517.70/477	537.35/477	480.07/477	451.54/477
Gain offset for SXT (E-02)	$3.04^{+0.007}_{-0.008}$	$3.83^{+0.005}_{-0.005}$	$3.99^{+0.006}_{-0.006}$	$3.87^{+0.008}_{-0.008}$

Γ is the powerlaw photon index of THCOMP. kT_e is the electron temperature of the Corona in keV. kT_{bb} is blackbody temperature in keV units. Energy band of 5.0-20.0 keV is taken for fitting of LAXPC 10 and 20 spectra and 0.7-6.0 for SXT spectrum.

time snaps in which LAXPC counters were also observing the source in each flux state. This is done by the XSELECT v2.4g tool. We have selected the SXT energy band 0.7-6.0 keV and fit it jointly with LAXPC spectra, as energies lower than 0.7 are avoided for uncertainties in the response. This led us to analyse data from the two instruments in a broad energy band of 0.7-20.0 keV, for each flux state.

We consider the LAXPC 20 unit's top layer spectra as the base spectra and accordingly its constant is pegged at 1. We adopt a two component model combination - $\text{Constant} \times \text{TBABS}(\text{THCOMP} + \text{GAUSS} + \text{BBODY})$ in XSPEC v12.10.1f, to model the four flux regions. A systematic error of 3% is considered to account for the response uncertainties for the two instruments (LAXPC and SXT), as per the guidelines of the SXT team. The SXT response spectrum is provided with a gain correction using a fixed slope of 1.0 and an offset, which is a free parameter.

A hump in the residuals at ~ 6 keV is observed. To improve our fitting, we add a Gaussian model GAUSS to BBODY and set the energy line freezed at ~ 6.4 keV. The thermally Comptonised model THCOMP is fitted for a covering fraction of 1, which assumes all the seed photons are Comptonised. No redshift value is provided. We have used the command "*energies 0.01 500 1000 log*" to extend the energy range with 1000 log bins for the model THCOMP.

We notice that our fitting has obtained the SXT constant values much lesser than LAXPC constants, which is explanatory to the fact that the SXT spectra is obtained after a pile up correction from a region with an annular cut. All the parameter values are tabularized in Table 3.2.

3. Probing the accretion flow properties of NS LMXB 4U 1608-52 using AstroSat observations

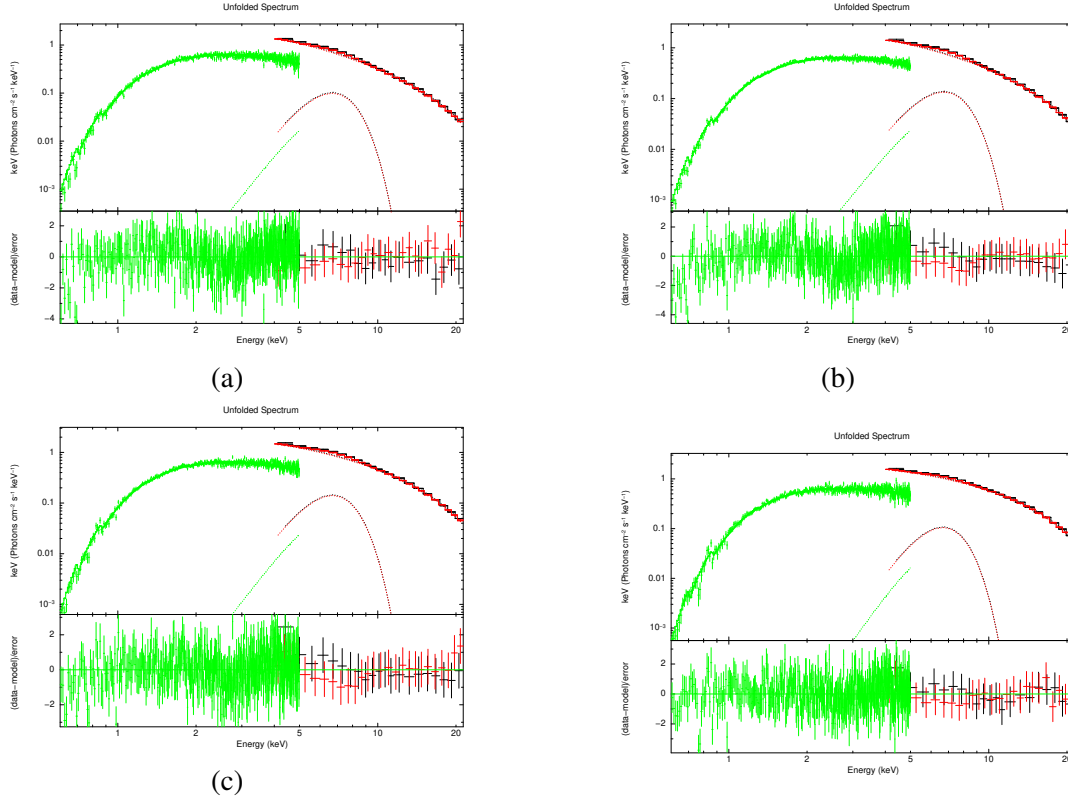


Figure 3.9: Flux resolved spectroscopy carried out using model combination $\text{Constant} \times \text{TBABS} \times (\text{GAUSS} + \text{THCOMP} \times \text{BLACKBODY})$. We have used LAXPC 10 (red), 20 (black) and SXT data (green). No redshift is considered. The THCOMP parameter photon convergence fraction is taken 100%. The spectral files are generated for the flux regions selected from the HID (see Fig. 3.5)

3.5 Discussions

We have investigated the X-ray binary 4U 1608-52 using data extracted from level 1 eventfiles from SXT and LAXPC instruments on-board. The major objective of this chapter is to analyse the steep correlation of Hardness Intensity with the source count rate. However, prior to this analysis, we have utilised the high resolution capability of LAXPC counters to do the timing analysis at central frequencies as low as 0.05 hz to 0.13 hz. We report that there is no time-lag of photons, at an average.

The main focus of this chapter is spectral modelling adopting flux resolved spectroscopy technique. The parametric changes observed for four flux states are 1. the photon index shows a negative correlation with flux, however the decrement is not steep and 2. the electron temperature of the corona is found to be approximately constant. Additionally, the blackbody temperature reported shows a decline beyond 4000 counts/s. We would like to introduce the relation between kT_e , Γ and τ below (Zdziarski, Johnson, & Magdziarz, 1996; Życki, Done, & Smith, 1999)

$$\tau = \sqrt{\left[\frac{9}{4} + \frac{3m_e c^2}{kT_e(\Gamma + 0.5)^2 - 9/4} \right]} - \frac{3}{2} \quad (3.1)$$

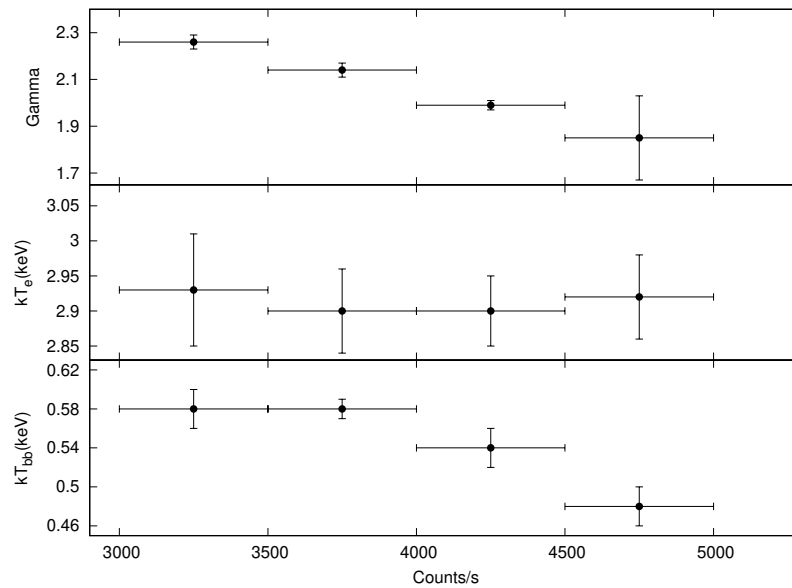


Figure 3.10: Evolution of spectral parameters with photon flux intensity in units of Counts/s selected from the Fig. 3.5. The photon index shows a decline whereas the electron temperature is fairly steady. The blackbody temperature shows a decline as well. No spectral correction factor is applied.

Plugging in the values of kT_e and Γ in this equation we observe that the optical depth τ shows a minor increment with the flux - from 0.05 to 0.07. We highlight here that Barua et al. (2020) has shown a similar evolution of the optical depth of AGN Ark 564, where the photon index was found to be approximately constant and the electron temperature to decrease with flux.

Flux estimation of SXT data

- The unabsorbed flux estimation of SXT using CFLUX model couldn't be performed for SXT with LAXPC counters due to some problems in cross-calibration. This needs to be sorted out.
- Due to this, SXT flux isn't reported in the manuscript.

Acknowledgements

Ankur Nath and Biplob Sarkar acknowledge the financial support of ISRO under AstroSat archival Data utilization program (No.DS_2B-13013(2)/2/2019-Sec.2). AN thanks the scholar mates from IUCAA, Pune who has helped sort out difficulties during the progress of the work. This work has utilized the softwares provided by HEASARC. In this work we have used data from the AstroSat mission of ISRO, archived at ISSDC.

Bibliography

- Agrawal V. K., Misra R., 2009, MNRAS, 398, 1352
- Agrawal V. K., Nandi A., Girish V., Ramadevi M. C., 2018, MNRAS, 477, 5437.
- Agrawal V. K., Nandi A., 2020, MNRAS, 497, 3726.
- Barua S., Jithesh V., Misra R., Dewangan G. C., Sarma R., Pathak A., 2020, MNRAS, 492, 3041.
doi:10.1093/mnras/staa067
- Beri A., Paul B., Yadav J. S., Antia H. M., Agrawal P. C., Manchanda R. K., Dedhia D., et al., 2019, MNRAS, 482, 4397.
- Bhulla Y., Roy J., Jaaffrey S. N. A., 2020, RAA, 20, 098.
- Chen W., Shrader C. R., Livio M., 1997, ApJ, 491, 312.
- Chen Y. P., Zhang S., Zhang S. N., Ji L., Kong L. D., Santangelo A., Qu J. L., et al., 2019, JHEAp, 24, 23.
- Chen X., Zhang S. N., Ding G. Q., 2006, ApJ, 650, 299.
- Church M. J., Inogamov N. A., Bałucińska-Church M., 2002, A&A, 390, 139.
- Di Salvo T., Iaria R., Burderi L., Robba N. R., 2000, ApJ, 542, 1034.
- Falanga M., Götz D., Goldoni P., Farinelli R., Goldwurm A., Mereghetti S., Bazzano A., et al., 2006, A&A, 458, 21
- Gierliński M., Done C., 2002, MNRAS, 337, 1373.
- Güver T., Özel F., Cabrera-Lavers A., Wroblewski P., 2010, ApJ, 712, 964
- Hasinger G., van der Klis M., 1989, A&A, 225, 79

Bibliography

- Kajava J. J. E., Koljonen K. I. I., Nätttilä J., Suleimanov V., Poutanen J., 2017, *MNRAS*, 472, 78.
- Kaaret P., Yu W., Ford E. C., Zhang S. N., 1998, *ApJL*, 497, L93.
- Farinelli R., Titarchuk L., 2011, *A&A*, 525, A102.
- Marshall F. E., Angelini L., 1996, *IAUC*, 6331
- Mitsuda K., Inoue H., Koyama K., Makishima K., Matsuoka M., Ogawara Y., Shibasaki N., et al., 1984, *PASJ*, 36, 741
- Mitsuda K., Inoue H., Nakamura N., Tanaka Y., 1989, *PASJ*, 41, 97
- Nakamura N., Dotani T., Inoue H., Mitsuda K., Tanaka Y., Matsuoka M., 1989, *PASJ*, 41, 617
- Piraino S., Santangelo A., Kaaret P., 2000, *A&A*, 360, L35
- Paizis A., Farinelli R., Titarchuk L., Courvoisier T. J.-L., Bazzano A., Beckmann V., Frontera F., et al., 2006, *A&A*, 459, 187.
- Šimon V., 2004, *A&A*, 418, 617.
- Suzuki K., Matsuoka M., Inoue H., Mitsuda K., Ohashi T., Tanaka Y., Hirano T., et al., 1984, *PASJ*, 36, 761
- Strohmayer, T. E., Altamirano, D., Arzoumanian, Z., et al. 2019, *ApJL*, 878, L27
- Tananbaum H., Chaisson L. J., Forman W., Jones C., Matilsky T. A., 1976, *ApJL*, 209, L125.
- White N. E., Stella L., Parmar A. N., 1988, *ApJ*, 324, 363.
- van Straaten S., van der Klis M., Méndez M., 2003, *ApJ*, 596, 1155.
- Yu W., Zhang S. N., Harmon B. A., Paciesas W. S., Robinson C. R., Grindlay J. E., Bloser P., et al., 1997, *ApJL*, 490, L153.
- Zhang S. N., Harmon B. A., Paciesas W. S., Fishman G. J., Grindlay J. E., Barret D., Tavani M., et al., 1996, *A&AS*, 120, 279
- Zdziarski A. A., Johnson W. N., Magdziarz P., 1996, *MNRAS*, 283, 193. doi:10.1093/mnras/283.1.193
- Zdziarski A. A., Szanecki M., Poutanen J., Gierliński M., Biernacki P., 2020, *MNRAS*, 492, 5234. doi:10.1093/mnras/staa159
- Życki P. T., Done C., Smith D. A., 1999, *MNRAS*, 309, 561. doi:10.1046/j.1365-8711.1999.02885.x

Chapter 4

Conferences and webinars attended

During the progress of the project, the PI and the JRF have attended a number of conferences and workshops, which are enlisted below

- The JRF attended the “3rd IUCCA sponsored Workshop on Astronomical Data Analysis” at J. B. College, Jorhat, Assam” in 2019.
- The JRF attended the IUCAA Sponsored Introductory Workshop on Physical Perspectives of Astronomy (IWPPA), October 30 - 31, 2019, Department of Physics, The ICFAI University Tripura. Coordinators: Biplob Sarkar & Gulab Chand Dewangan
- The JRF has presented a poster in “Royal Astronomical Society Early Career Poster Exhibition” in 2020.
- The PI delivered a lecture on “Detection of a Type-I X-ray thermonuclear burst from GX 3+1 through AstroSat” in North East Meet of Astronomers (NEMA)-VI, November 10-13, 2020, organized by the Department of Physics, IIT Guwahati.
- The JRF presented an oral presentation in “National Seminar on Recent Advances in Astrophysics and Cosmology” held by North Bengal University, 2021.
- The PI participated and presented an Oral Paper entitled “AstroSat observation of rapid Type-I thermonuclear burst from the low mass X-ray binary GX 3+1” in the National Conference on Emerging Trends in Physics (NCETP 2021) organized by Department of Physics, Tezpur University, Assam, India held on 16 June, 2021.
- The PI presented a poster entitled “AstroSat observations of the transient low-mass X-ray binary 4U 1608-52” in Two-days International Conference on Innovative Trends in Natural

4. *Conferences and webinars attended*

and Applied Sciences - 2021 (ICITNAS - 2021) organized by Mahatma Gandhi College Of Science, Gadchandur, Tah. Korpana, Dist. Chandrapur- 442908 (M.S.), India on 17 -18 August, 2021.

- The PI participated and presented an Oral Paper entitled “Probing the accretion flow properties of NS LMXB 4U 1608-52 using AstroSat observations”, Biplob Sarkar, in 21st National Space Science Symposium, January 31 - February 4, 2022, organized by IISER Kolkata, India.
- The PI presented a poster entitled “Broad-band spectral and temporal characteristics of NS LMXB 4U1608-52 through AstroSat observations” in the 40th Annual Meeting of the Astronomical Society of India (ASI), hosted jointly by IIT Roorkee and ARIES Nainital during 25-29 March 2022.

GFR 12 - A
(See Rule 238(1))
FORM OF UTILISATION CERTIFICATE
FOR GRANTEE ORGNISATION

UTILISATION FOR THE YEAR 2020-2021 in respect of GRANTS-IN-AID Released by Department of Space

1. Project title: Investigation of the accretion flow properties of black hole binaries with AstroSat

2. Name of the PI & Designation: Dr. Biplob Sarkar (Assistant Professor)

3. Name & Address of the Institution: Tezpur University, Napaam, Sonitpur, Assam-784 028, INDIA

4. Name of the Scheme: "Announcement of Opportunity Proposal for Utilizing AstroSat archival data" Space Sciences (2792)

5. Whether recurring or no recurring grants: Recurring grants

6. Grants position at the beginning of the Financial year

(i) Cash in Hand/Bank	NIL
(ii) Unadjusted advances	0.00
(iii) Total	NIL

7. Details of grants received, expenditure incurred and closing balances:(Actuals) Rs. Cr.

Unspent Balances of grants received years (Figure as at Sl. No 3(iii))	Interest earned thereon	Interest deposited back to the Government	Grant received during the year			Total available Fund (1+2-3+4)	Expenditure incurred	Closing Balances (5-6)
			Sanction No. (i)	Date (ii)	Amount (iii)			
1	2	3	4			5	6	7
0.00	567.00	0.00	No.DS_2B-13013(2)/2/2019-Sec.2	30.12.2020	1,30,462.00	1,31,029.00	38,502.00	92,527.00

Details of Grant position at the end of the year

(i) Cash in Hand/Bank	92,527.00
(ii) Unadjusted advances	NIL
(iii) Total	92,527.00

Certified that I have satisfied myself that the conditions on which grants were sanctioned have been duly fulfilled/are being fulfilled and that I have exercised following checks to see that the money has been actually utilized for the purpose for which it was sanctioned:

- i. The main accounts and the other subsidiary accounts and registers (including assets registers) are maintained as prescribed in the relevant Act/Rules/Standing instructions (mentioned the Act/Rules) and have been duly audited by designated auditors. The figures depicted above tally with the audited figures mentioned in financial statements/accounts.
- ii. There exist internal controls for safeguarding public funds/assets, watching outcomes and achievements of physical targets against the financial inputs, insuring quality in asset creation etc. & the periodic evaluation of internal controls is exercised to ensure their effectiveness.
- iii. To the best of our knowledge and belief, no transactions have been entered that are in violation of relevant Act/Rules/Standing instructions and scheme guidelines.
- iv. The responsibilities among the key functionaries for execution of the scheme have been assigned in clear terms and are not general in nature.
- v. The expenditure on various components of the scheme was in proportions authorized as per the scheme guidelines and terms and conditions of the grants-in-aid.
- vi. It has been ensured that the physical and financial performance under the scheme "Investigation of the accretion flow properties of black hole binaries with AstroSat" reg. has been according to the requirements, as prescribed in the guidelines issued by Govt. of India and the performance /targets achieved statement for the year to which the utilization of the fund resulted in outcomes given at Reports submitted to the Programme Office.
- vii. The utilization of the fund resulted in outcomes given at Reports duly forwarded to respective programme Office (to be formulated by the Department concerned as per their requirements/specifications).
- viii. Details of various schemes executed by the agency through grants-in-aid received from the same Ministry or from other Ministries is enclosed at Annexure
- ix. It is certified that for the same purpose we have not received any grant from the other Ministry/Department or any other Private Body.

Date: 30/08/22

Place: Napaam, Tezpur

Signature

Name.....

Chief Finance Officer (Head of the Finance)

Seal

Finance Officer
Tezpur University

Signature

Name.....

Head of the Organisation

Seal

Registrar
Tezpur University

Signature

Name DR. BIPLOB SARKAR

30/08/22

DEPARTMENT OF APPLIED SCIENCES, TEZPUR UNIVERSITY
Project PI

Note: Any interest earned on unutilized funds during previous year and not remitted back to Govt. should be included in the opening balance at Sl. No. 3 (i)

GFR 12 - A
(See Rule 238(1))
FORM OF UTILISATION CERTIFICATE
FOR GRANTEE ORGNISATION

UTILISATION FOR THE YEAR 2021-2022 in respect of GRANTS-IN-AID Released by Department of Space

1. Project title: Investigation of the accretion flow properties of black hole binaries with AstroSat
2. Name of the PI & Designation: Dr. Biplob Sarkar (Assistant Professor)
3. Name & Address of the Institution: Tezpur University, Napaam, Sonitpur, Assam-784 028, INDIA
4. Name of the Scheme: "Announcement of Opportunity Proposal for Utilizing AstroSat archival data" Space Sciences (2792)
5. Whether recurring or no recurring grants: Recurring grants
6. Grants position at the beginning of the Financial year
- | | |
|--------------------------|-----------|
| (i) Cash in Hand/Bank | 92,527.00 |
| (ii) Unadjusted advances | NIL |
| (iii) Total | 92,527.00 |

7. Details of grants received, expenditure incurred and closing balances:(Actuals) Rs. Cr.

Unspent Balances of grants received years (Figure as at Sl. No 3(iii))	Interest earned thereon	Interest deposited back to the Government	Grant received during the year			Total available Fund (1+2-3+4)	Expenditure incurred	Closing Balances (5-6)
			Sanction No. (i)	Date (ii)	Amount (iii)			
1	2	3	4			5	6	7
92,527.00	1,425.00	0.00	No.DS_2B-13013(2)/2/2019-Sec.2	24.12.2021	3,46,836.00	4,40,788.00	2,70,499.00	1,70,289.00

Details of Grant position at the end of the year


(i) Cash in Hand/Bank	1,70,289.00
(ii) Unadjusted advances	NIL
(iii) Total	1,70,289.00

Certified that I have satisfied myself that the conditions on which grants were sanctioned have been duly fulfilled/are being fulfilled and that I have exercised following checks to see that the money has been actually utilized for the purpose for which it was sanctioned:

- i. The main accounts and the other subsidiary accounts and registers (including assets registers) are maintained as prescribed in the relevant Act/Rules/Standing instructions (mentioned the Act/Rules) and have been duly audited by designated auditors. The figures depicted above tally with the audited figures mentioned in financial statements/accounts.
- ii. There exist internal controls for safeguarding public funds/assets, watching outcomes and achievements of physical targets against the financial inputs, insuring quality in asset creation etc. & the periodic evaluation of internal controls is exercised to ensure their effectiveness.
- iii. To the best of our knowledge and belief, no transactions have been entered that are in violation of relevant Act/Rules/Standing instructions and scheme guidelines.
- iv. The responsibilities among the key functionaries for execution of the scheme have been assigned in clear terms and are not general in nature.
- v. The expenditure on various components of the scheme was in proportions authorized as per the scheme guidelines and terms and conditions of the grants-in-aid.
- vi. It has been ensured that the physical and financial performance under the scheme "Investigation of the accretion flow properties of black hole binaries with AstroSat"- reg. has been according to the requirements, as prescribed in the guidelines issued by Govt. of India and the performance /targets achieved statement for the year to which the utilization of the fund resulted in outcomes given at Reports submitted to the Programme Office.
- vii. The utilization of the fund resulted in outcomes given at Reports duly forwarded to respective programme Office (to be formulated by the Department concerned as per their requirements/specifications).
- viii. Details of various schemes executed by the agency through grants-in-aid received from the same Ministry or from other Ministries is enclosed at Annexure
- ix. It is certified that for the same purpose we have not received any grant from the other Ministry/Department or any other Private Body.


Date: 30/08/22

Place: Napaam, Tezpur

Signature 
Name.....29/2

Chief Finance Officer (Head of the Finance)

Seal *Finance Officer*
Tezpur University

Signature 
Name.....05/09/22

Head of the Organisation

Seal *Registrar*
Tezpur University

Signature *Biplob Sarkar* 30/08/2022
Name DR. BIPLOB SARKAR
DEPARTMENT OF APPLIED SCIENCES, TEZPUR UNIVERSITY
Project PI

Note: Any interest earned on unutilized funds during previous year and not remitted back to Govt. should be included in the opening balance at Sl. No. 3 (i)

Audited Accounts Statement

1. Project Title : **Investigation of the accretion flow properties of black hole binaries with AstroSat**
2. Name of the PI & Designation : **Dr. Biplob Sarkar (Assistant Professor)**
3. Name & Address of University /Institution : **TEZPUR UNIVERSITY, NAPAAM, TEZPUR, ASSAM-784028**
4. ISRO/DOS Letter/Sanction order No & date : **No. DS-2B-13013(2)/2/2019-Sec.2 Dated April 23, 2019**
5. Period of Statement : **11-NOV-2020 TO 22-AUG-2022**
6. Total Grants Approved/ Grants for the Year : **Rs 4,77,298.00 (Total grant for second year project received by Tezpur University)**

Rs. 1,30,462.00 (First quarter grant for second year project received by Tezpur University on 30/12/2020)

Rs. 3,46,836.00 (Balance grant of second year project received by Tezpur University on 24/12/2021)
7. University/Institution Sanction No. and Date : **DoRD/ASc./BS/20-477 Dated 19/01/2021**
8. Expenditure Statement for the Period : **11-NOV-2020 TO 22-AUG-2022**

(D in lakhs)

Sl. No	Budget Item	Grant released by ISRO/DOS	Expenditure incurred	Unspent balance	Remarks
1	FUND	Rs 1,30,462/-			Received on 30/12/2020
2	FUND	Rs 3,46,836/-			Received on 24/12/2021
3	FELLOWSHIP		Rs 3,03,449/-		
4	CONTINGENCY		Rs 5,552/-		
5	INTEREST EARNED				Rs 1,992/- (For the period 11-NOV-2020 To 22-AUG-2022)
6				Rs 1,70,289/-	As on 22-Aug-2022

Place: **Napaam, Tezpur**

Date: **30/08/2022**

Biplob Sarkar
30/08/22
Dr. Biplob Sarkar
Assistant Professor
Department of Applied Sciences
Tezpur University
Napaam, Tezpur-784028, Assam
Principal Investigator
(with seal)

Biplob Sarkar
Head of the Institution
(with Seal)
Registrar
Tezpur University

[Signature]
Finance Officer/Registrar
(with Seal)
Finance Officer
Tezpur University

Auditor
(with Seal)